


Article

What Are the Variation Patterns of Vegetation and Its Influencing Factors in China from 2000–2020 from the Partition Perspective?

Bing Guo ¹, Mei Xu ¹, Rui Zhang ^{2,*}, Wei Luo ^{3,*}  and Jicun Yang ¹

¹ School of Civil Engineering and Geomatics, Shandong University of Technology, Zibo 255000, China; guobing@sdut.edu.cn (B.G.); 22407010008@stumail.sdut.edu.cn (M.X.); 23507020861@stumail.sdut.edu.cn (J.Y.)

² Key Laboratory of Remote Sensing of Gansu Province, Heihe Remote Sensing Experimental Research Station, Northwest Institute of Eco-Environment and Resources, Chinese Academy of Sciences, Lanzhou 730000, China

³ School of Remote Sensing and Information Engineering, North China Institute of Aerospace Engineering, Langfang 065000, China

* Correspondence: zhangrui@radi.ac.cn (R.Z.); luowei@radi.ac.cn (W.L.)

Abstract: China's vegetation ecosystem has undergone profound changes, and there is an urgent need to explore the mechanisms behind vegetation changes in different ecological sub-regions and historical periods across China. Based on NDVI (normalized difference vegetation index) data, this study analyzed the spatial and temporal evolution patterns and driving mechanisms of six ecological sub-regions in China. The results showed that: (1) over the past 20 years, the vegetation coverage in mainland China showed a decreasing trend from east to west. (2) Over the past 20 years, the vegetation coverage of the six ecological sub-regions showed an increasing trend, with the highest increase in Central Southern China (0.0039) and the lowest increase in East China (0.002). (3) The gravity center of Northeast China showed a trend of migration to the northwest. The gravity center of North China, East China, and Central South China showed a trend of migration to the southwest, while that of Northwest and Southwest China showed a trend of migration to the southeast. (4) During the period from 2000 to 2020, vegetation cover levels showed an upward trend. (5) The lag time of vegetation types in different regions was different. (6) Precipitation was the dominant influencing factor in the evolution of vegetation in Northeast China, North China, Northwest China, and Southwest China. The dominant influencing factors of vegetation evolution in East China were land use and GDP (gross domestic product), while the dominant influencing factors of vegetation evolution in Central South China were precipitation and land use.

Keywords: China; NDVI; vegetation coverage; time lag effect; gravity center



Citation: Guo, B.; Xu, M.; Zhang, R.; Luo, W.; Yang, J. What Are the Variation Patterns of Vegetation and Its Influencing Factors in China from 2000–2020 from the Partition Perspective? *Forests* **2024**, *15*, 1409. <https://doi.org/10.3390/f15081409>

Academic Editors: Gilson Alexandre Ostwald Pedro da Costa, Raul Queiroz Feitosa, Veraldo Liesenberg and Claudio Almeida

Received: 2 July 2024

Revised: 7 August 2024

Accepted: 9 August 2024

Published: 11 August 2024



Copyright: © 2024 by the authors. Licensee MDPI, Basel, Switzerland. This article is an open access article distributed under the terms and conditions of the Creative Commons Attribution (CC BY) license (<https://creativecommons.org/licenses/by/4.0/>).

1. Introduction

Vegetation, as a representative of surface habitat conditions, plays a crucial role in regulating the ecological balance of watershed ecosystems, and it also has significant effects on hydrological and geomorphological processes [1]. Vegetation growth is highly sensitive to environmental changes and is regarded as an ‘indicator’ of global change [2]. Vegetation is also a natural link connecting the atmosphere, hydrosphere, and soil, and it plays a vital role in soil and water conservation, climate, and ecological stability [3]. The growth of terrestrial vegetation is affected not only by climate change but also by human activities. In recent years, with the intensification of phenomena such as global warming, urban expansion, and population growth, vegetation changes have also been affected to a certain extent. An in-depth analysis of the spatial and temporal variation characteristics of vegetation and its influencing factors is of great significance for achieving the goal of ‘double carbon’ and maintaining ecological balance.

In recent years, numerous scholars have conducted analyses on vegetation coverage and driving mechanisms in different regions based on remote sensing imagery data. However, previous studies have had limited discussion on transitions between different levels, and most of the correlation analyses have used first-order partial correlation as the analytical tool. Lu et al. (2024) conducted a study on the impact of meteorological drought and hydrological drought on vegetation NDVI changes in the Inner Mongolia section of the Yellow River Basin, using the standardized precipitation evapotranspiration index (SPEI) dataset and terrestrial water storage data. However, the study did not explore transitions between the two levels, and the correlation analysis employed the first-order partial correlation method [4]. Wang et al. (2024), based on Landsat data and using the salinity index (SI), introduced the modified remote sensing ecological index (MRSEI). They combined it with landscape indices and employed spatial autocorrelation analysis methods. Through the use of geographical detectors, they conducted a driving factor analysis to quantitatively evaluate the spatiotemporal differentiation characteristics of the ecological environment in the Sanjiang Plain of the Yellow River. The first-order partial correlation was also used as the analytical tool [5]. Shen et al. (2024), based on the NDVI, utilized slope-trend analysis and the coefficient of variation to analyze vegetation cover changes in the Hexi Inland River Basin from 2000 to 2020. However, they did not explore transitions between different levels [6]. Mason et al.'s (2022) study on vegetation dynamics in Australia, based on MODIS NDVI data, indicates a trend of vegetation first decreasing and then increasing in the study area [7]. Vahagn et al. (2019) studied the characteristics and growth lag of vegetation changes in the mountainous regions of Armenia. They found that the period with the highest NDVI coincides with the vegetation growing season and that vegetation changes exhibit a lagged response to climate changes [8]. Therefore, this study innovatively applied the transition matrix technique to precisely quantify the detailed changes in the vegetation NDVI across different levels, thereby deepening the understanding of the dynamic evolution of the vegetation NDVI over time. Unlike the first-order partial correlation method, this study employed the second-order partial correlation coefficient, which provides a better approach for correlation analysis. Additionally, this study addressed the limitation of previous research that focused predominantly on ecologically fragile areas and lacked comprehensive national-scale investigations. By adopting a strategy of regional subdivision, it systematically explored the spatiotemporal variations in the vegetation NDVI and the fundamental drivers of these changes, enhancing the specificity and practical value of the research.

Based on the MODIS NDVI time series dataset, this study employed the gravity center model, time-lag effect analysis method, partial correlation analysis, and geographic detector to investigate the spatial and temporal evolution patterns of the vegetation NDVI in various ecological sub-regions of China, categorized by zoning. The study analyzed time lags and identified dominant driving factors influencing changes in the vegetation NDVI. These findings provide crucial decision support for the protection and restoration of regional vegetation ecosystems.

2. Materials and Methods

2.1. Overview of the Study Area

As depicted in Figure 1, China is situated in eastern Asia, along the western coast of the Pacific Ocean. It extends eastward to the confluence of the Heilongjiang and Wusuli Rivers ($135^{\circ}2'30''$ E), westward to the Pamirs ($73^{\circ}29'59.79''$ E), southward to the southernmost point of Hainan Island ($3^{\circ}31'00''$ N), and northward to the center line of the main channel of the Heilongjiang River ($53^{\circ}33'$ N) north of the Mohe River. China has a land area of 9.6 million km^2 . (Figure 1) and a coastline stretching 18,000 km. China's terrain is high in the west and low in the east, showing a three-stage ladder-like distribution. The five basic terrains of plateau, mountains, plains, hills, and basins are distributed in China. Due to the vast land area and the large span of latitude and longitude (north and south across the latitude of 50° , east and west across the longitude of 60°), the combination of temperature

and precipitation is diverse and constitutes a complex and diverse climate environment, among which the monsoon climate is the most significant, which also makes China often have meteorological disasters and geological disasters. Due to the large span of latitude between the north and the south, the spatial heterogeneity of temperature between the north and the south is obvious. South of the Qinling–Huaihe line, the region is primarily characterized by subtropical and tropical climates. To the north, including both sides of the Greater Khingan Mountains, the climate transitions to cold temperate zones. The area between these zones is predominantly in the temperate zone, with significant geographic expanse. Influenced by the southeast monsoon, precipitation decreases progressively from southeast to northwest across the region. The southeast coastal area will be the first to get the water vapor brought by the monsoon, forming rich precipitation, while the southwest region is deep inland, making less water vapor and less precipitation. The vegetation types are rich, mainly including grassland, tropical rainforest, evergreen broad-leaved forest, deciduous broad-leaved forest, and coniferous forest. The broad-leaved forest is widely distributed in temperate and warm temperate regions, and the coniferous forest is mainly distributed in cold temperate regions. China's terrain is characterized by higher elevations in the west and lower elevations in the east, forming a distinct step-like distribution. The northeast region is dominated by temperate needleleaf and mixed forests. In North China, deciduous broadleaf forests prevail, primarily composed of species such as oak, birch, poplar, elm, and maple. The eastern region falls within the zone of warm-temperate deciduous broadleaf forests, typical of the subtropical evergreen broadleaf forest zone of Central Asia, and so on. The soil types are complex and diverse, and the distribution changes regularly with the change of geographical location and terrain height. It is not only manifested as horizontal zonality but also related to vertical zonality and regionality.

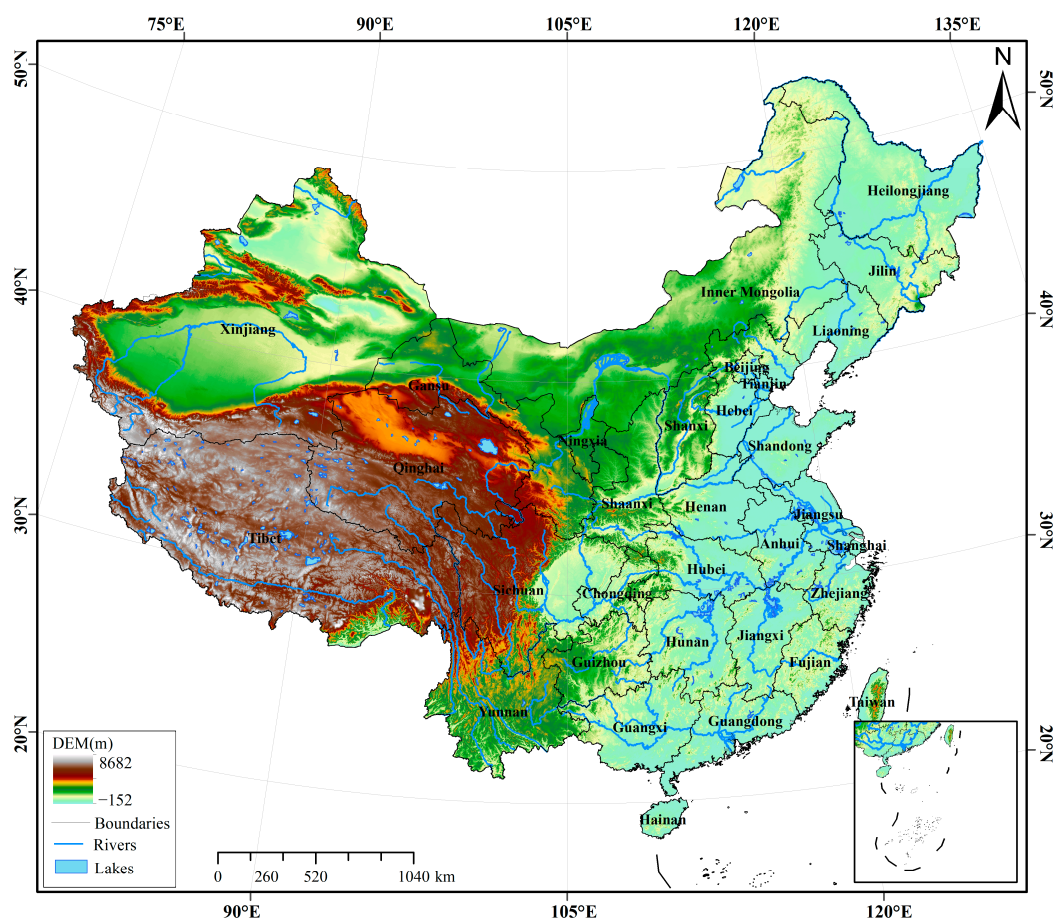


Figure 1. Overview of study area.

2.2. Data Source and Preprocessing

The NDVI vegetation data and vegetation type data used in this study are sourced from the National Tibetan Plateau Data Center (<https://data.tpdc.ac.cn/zh-hans/data/>, accessed on 20 December 2023). The NDVI dataset was created by Landsat satellites, originally in TIFF format, with a spatial resolution of 250 m and temporal resolution at a monthly scale, covering the period from 2000 to 2020. The vegetation type data are in vector format and was converted to TIFF format using the Polygon to Raster tool in ArcGIS 10.7. The data from climate observation stations were collected from the China Meteorological Administration Data Service Center (<http://data.cma.cn/>, accessed on 22 December 2023), encompassing approximately 800 widely distributed ground-based meteorological stations across China (See Figure 2). These records include key indicators such as annual precipitation, annual average temperature, cumulative temperature, and annual sunshine hours. Interpolation to obtain 1 km grid data was performed using the Geostatistical Analyst tool in ArcGIS 10.7. Land use data, socio-economic data (population density, GDP), and six major zoning data are derived from the Resource and Environmental Science and Data Center of the Chinese Academy of Sciences (<http://www.resdc.cn/DOI/>, accessed on 23 December 2023). The time resolution is 1 year, in which the spatial resolution of land use data is 30 m, and the spatial resolution of socio-economic data is 1 km. The elevation and slope data are extracted from SRTM90m, and the data are derived from the geospatial data cloud (<http://www.Gscloud.cn>, accessed on 27 December 2023). The above data sets all use ArcGIS10.7 to eliminate, clip, resample (1 km), and re-project (SIN projection→Krasovski projection) data outliers.

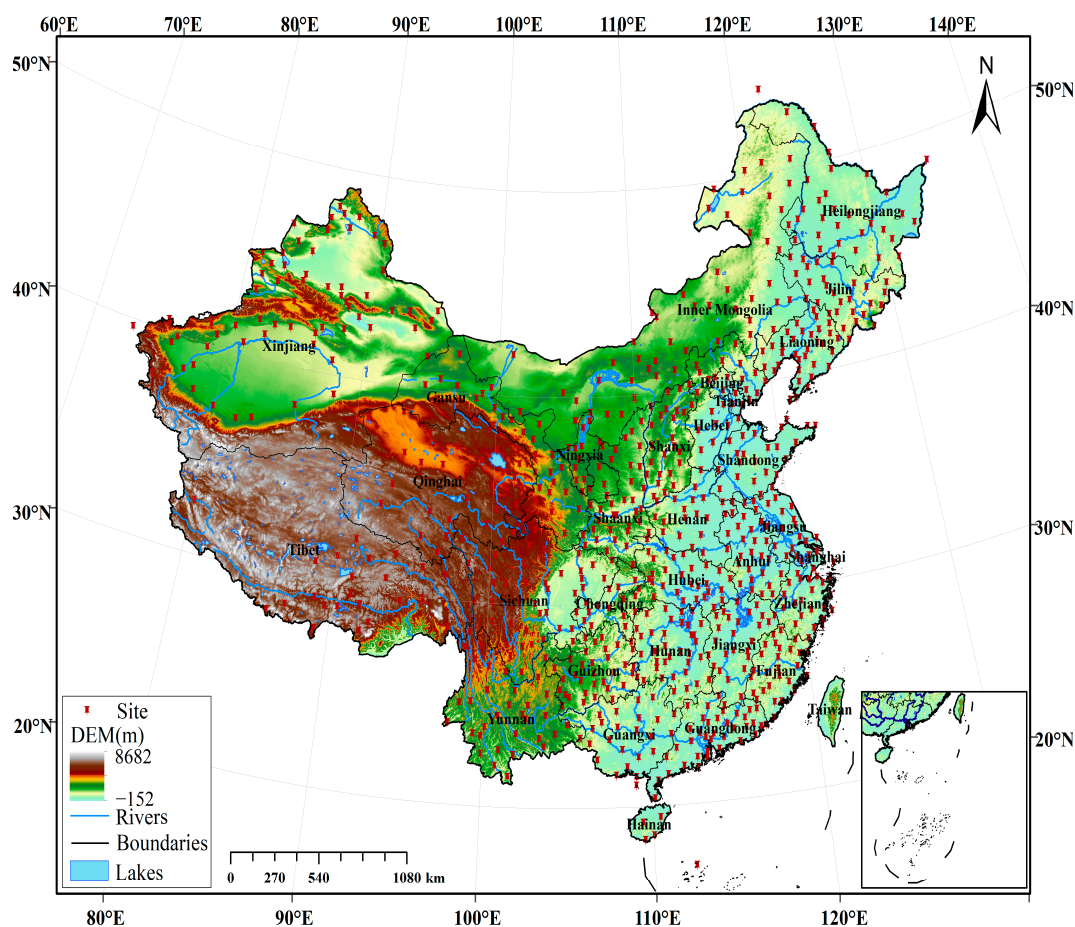


Figure 2. The distribution of meteorological stations in China.

2.3. Research Methods

2.3.1. Gravity Center Model

In physics, the center of gravity refers to a point within a specific area of space where the forces acting in all directions achieve a state of equilibrium. This point represents the average location of the gravitational forces exerted on an object or within a system [9]. In addition to the field of physics, the gravity center has also been widely used in people's production, lives, land use, and other fields. The formula is as follows:

$$\begin{aligned}\bar{x} &= \frac{\sum_{i=1}^n z_i x_i}{\sum_{i=1}^n z_i} \\ \bar{y} &= \frac{\sum_{i=1}^n z_i y_i}{\sum_{i=1}^n z_i}\end{aligned}\quad (1)$$

In the formula, (\bar{x}, \bar{y}) is the latitude and longitude coordinates of the center of gravity of an NDVI spatial distribution in the n th year, z_i is the area of the i th patch of the NDVI in the n th year, and (x_i, y_i) is the latitude and longitude coordinates of the center of gravity of the i patch of the NDVI.

The gravity center migration direction can characterize areas with larger NDVI values, and the gravity center migration distance can reveal the dispersion degree of the gravity center distribution of the vegetation NDVI. The calculation formula is as follows:

$$\begin{aligned}\theta &= \arctan\left(\frac{y_{t+m} - y_t}{x_{t+m} - x_t}\right) \\ d &= \sqrt{(y_{t+m} - y_t)^2 + (x_{t+m} - x_t)^2}\end{aligned}\quad (2)$$

In the formula, θ is the migration angle of the gravity center of the vegetation NDVI, d is the migration distance of the gravity center of the vegetation NDVI, y_{t+m} and y_t represent the ordinate of the gravity center at $t + m$ and t , respectively, and x_{t+m} and x_t represent the abscissa of the gravity center at $t + m$ and t , respectively.

2.3.2. Correlation Analysis

The correlation coefficient can characterize the degree of correlation between different elements [10]. The calculation formulas of the Pearson correlation coefficient and partial correlation coefficient are as follows:

$$r_{x,y} = \frac{\sum_{i=1}^n (x_i - \bar{x})(y_i - \bar{y})}{\sqrt{\sum_{i=1}^n (x_i - \bar{x})^2 \sum_{i=1}^n (y_i - \bar{y})^2}}, \quad (3)$$

$$r_{xy_1, y_2} = \frac{r_{xy_1} - r_{xy_2} r_{y_1, y_2}}{\sqrt{1 - r_{x, y_2}^2} \sqrt{1 - r_{y_1, y_2}^2}}. \quad (4)$$

In the formula, r_{xy} represents the correlation coefficient of the x variable and y variable (r_{xy_1} , r_{xy_2} , and r_{y_1, y_2} are similar), where a positive value represents a positive correlation. r_{xy_1, y_2} represent the values of the two variables in the i year, respectively. Represents the partial correlation coefficient of x and y_1 in the case of control variables.

When controlling multiple variables, there are high-order partial correlation coefficients. The formula is as follows:

$$r_{xy,y_1y_2\dots y_g} = \frac{r_{xy,y_1y_2\dots y_{g-1}} - r_{xy_g,y_1y_2\dots y_{g-1}}r_{yy_g,y_1y_2\dots y_{g-1}}}{\sqrt{1 - r_{xy_g,y_1y_2\dots y_{g-1}}^2} \sqrt{1 - r_{yy_g,y_1y_2\dots y_{g-1}}^2}} \tag{5}$$

The partial correlation coefficient is tested by the T significance test, and the significance test formula is as follows:

$$t = \frac{r}{\sqrt{1 - r^2}} \sqrt{n - m - 1}, \tag{6}$$

where r represents the partial correlation coefficient, n is the number of samples, and m is the number of variables.

In this study, the second-order partial correlation coefficient was used to test the significance of the vegetation NDVI at $p < 0.05$ and $p < 0.01$ confidence levels.

2.3.3. Trend Analysis

The trend of the NDVI in China from 2000 to 2020 was analyzed by linear regression [11]. The calculation formula is as follows:

$$\theta_{slope} = \frac{n \times \sum_{i=1}^n i \times NDVI_i - \sum_{i=1}^n i \sum_{i=1}^n NDVI_i}{n \times \sum_{i=1}^n i^2 - \left(\sum_{i=1}^n i\right)^2} \tag{7}$$

In the formula, i denotes the year, n is the number of years of time series, $NDVI_i$ is the NDVI of the first year, and the slope is the slope of the trend line. When the value is positive or negative, it indicates that the vegetation NDVI changes with time and shows an improvement or degradation trend. If slope > 0 , it means that the NDVI of vegetation has increased. If slope < 0 , it indicates that the vegetation NDVI is decreasing.

The F test was used to test the significance of the change trend [12]. The calculation formula is as follows:

$$F = U \times \frac{n - 2}{Q}, \tag{8}$$

$$U = \sum_{i=1}^n (\hat{y}_i - \bar{y}), \tag{9}$$

$$Q = \sum_{i=1}^n (y_i - \hat{y}_i)^2 \tag{10}$$

In the formula, Q is the regression sum of squares, which is the sum of the squared deviations of the regression values of the dependent variable from the mean of the dependent variable. U is the sum of squares of residuals \hat{y}_i is the fitted regression value of the NDVI, \bar{y} is the mean NDVI over n years, y_i is the NDVI value for the i th year, and n is the number of years.

As shown in Table 1, according to the slope and the significance level, the vegetation NDVI growth is divided into five levels.

Table 1. Significant classification.

Change Type	F Test Significance Level	NDVI Change Slope
Obviously increased	$p \leq 0.05$	$k \geq 0.001$
Little increase	$0.05 < p \leq 0.1$	$k \geq 0.001$
Essentially constant	$p > 0.1$	$-0.001 < k < 0.001$
Slightly reduced	$0.05 < p \leq 0.1$	$k \leq -0.001$
Decreased significantly	$p \leq 0.05$	$k \leq -0.001$

2.3.4. Geographical Detector

The geographical detector model can reveal the explanatory power of a factor to the vegetation NDVI [13]. The formula is as follows:

$$q = 1 - \frac{SSW}{SST}, \quad (11)$$

$$SSW = \sum_{h=1}^L N_h \sigma_h^2, \quad (12)$$

$$SST = N \sigma^2. \quad (13)$$

In the formula, $h = 1, \dots, L$ is the classification of variable Y or factor X , N_h and N are the layer h and the number of units in the whole region, respectively, σ_h^2 is the variance of the Y value of the class h , σ^2 is the variance of the Y value of the whole region, SSW is the sum of intra-layer variance, and SST is the total variance of the whole region.

3. Results

3.1. Spatial Distribution Pattern of Vegetation in China over the Past 20 Years

The annual NDVI during 2000–2020 was obtained (Figure 3), which was divided into five grades by equal interval method.

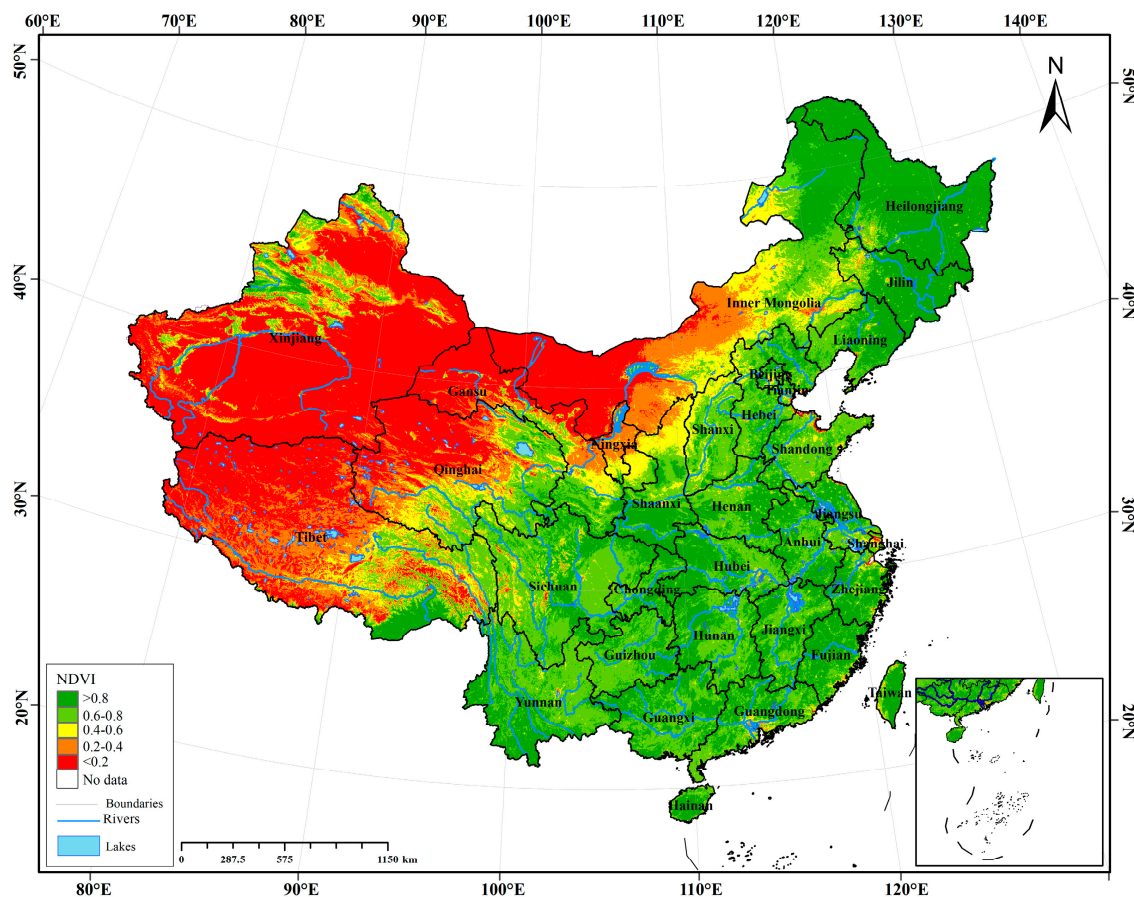


Figure 3. Spatial distributions of different levels of NDVI.

Based on Figure 3, the analysis reveals that the medium-high vegetation coverage area constituted the largest proportion, amounting to 28.3%. This region predominantly spans the third step of China, including provinces like Heilongjiang, Jilin, and Fujian. Conversely, areas characterized by low vegetation coverage in China accounted for the

second-highest proportion at 26.2%. These areas are primarily concentrated in regions such as the Taklimakan Desert, the western Qinghai-Tibet Plateau, and the Badain Jaran Desert. The area of high vegetation coverage accounted for 25%, mainly distributed in southern China, such as Hunan Province and Yunnan Province. The proportion of medium-low vegetation coverage and median vegetation coverage area was smaller, with 10.8% and 9.8%, respectively, mainly distributed in the Inner Mongolia Plateau and other areas at the junction of the second and third steps. From east to west, the vegetation coverage rate gradually decreased. Additionally, from north to south, the vegetation coverage showed a change from high vegetation coverage to a mixed distribution of high and medium-high vegetation coverage.

3.2. Temporal Variations of Vegetation in China at Different Time Scales over the Past 20 Years

3.2.1. Mean Change in Different Partitions

The average annual vegetation NDVI in each sub-region from 2000 to 2020 was counted and analyzed by a line chart, as shown in Figure 4.

As shown in Figure 4a, from 2000 to 2020, the NDVI fitting value of vegetation in Northeast China increased by 0.0038, showing a trend of increasing volatility as a whole. The goodness of fit R^2 was 0.7655, and the increase was more significant. The average annual maximum value appeared in 2018, which was 0.851, and the lowest value appeared in 2000, which was 0.756. The highest increase was 0.024 during 2009–2010, and the highest decrease was 0.033 during 2008–2009. By analyzing these fluctuations, it can be observed that the vegetation NDVI in the northeast region undergoes significant peaks and troughs approximately every three years. Since 2010, the NDVI values in the northeast have tended to stabilize, with the main fluctuation range between 0.82 and 0.84. Overall, over the past 21 years, the annual average vegetation NDVI in the northeast region has experienced complex changes, including growth, decline, and stability.

As shown in Figure 4b, during 2000–2020, the NDVI fitting value of vegetation in North China increased by 0.0034, showing an increasing trend of fluctuation. The goodness of fit R^2 was 0.5753, which was the lowest among the six regions, and the growth trend was more significant. The average annual maximum value appeared in 2018, which was 0.566, and the average annual minimum value appeared in 2001, which was 0.462. The highest increase was 0.038 during 2011–2012, and the highest decrease was 0.0274 during 2018–2019. Prior to 2015, this region did not exhibit significant peaks. However, since 2015, there have been notable peaks in consecutive years (2016 and 2018). Additionally, the observed gradual increase in the average values of interval numbers shows a segmented upward staircase-like change, further confirming the dynamic evolution characteristics of vegetation cover in North China.

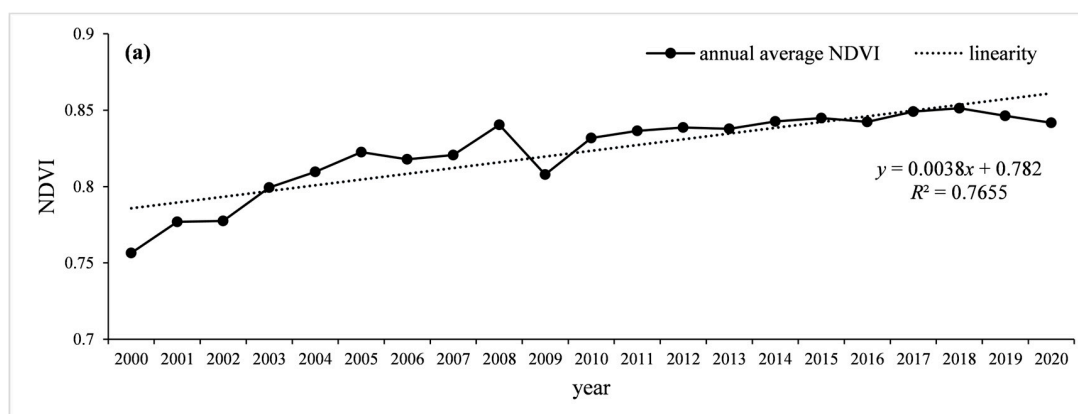


Figure 4. Cont.

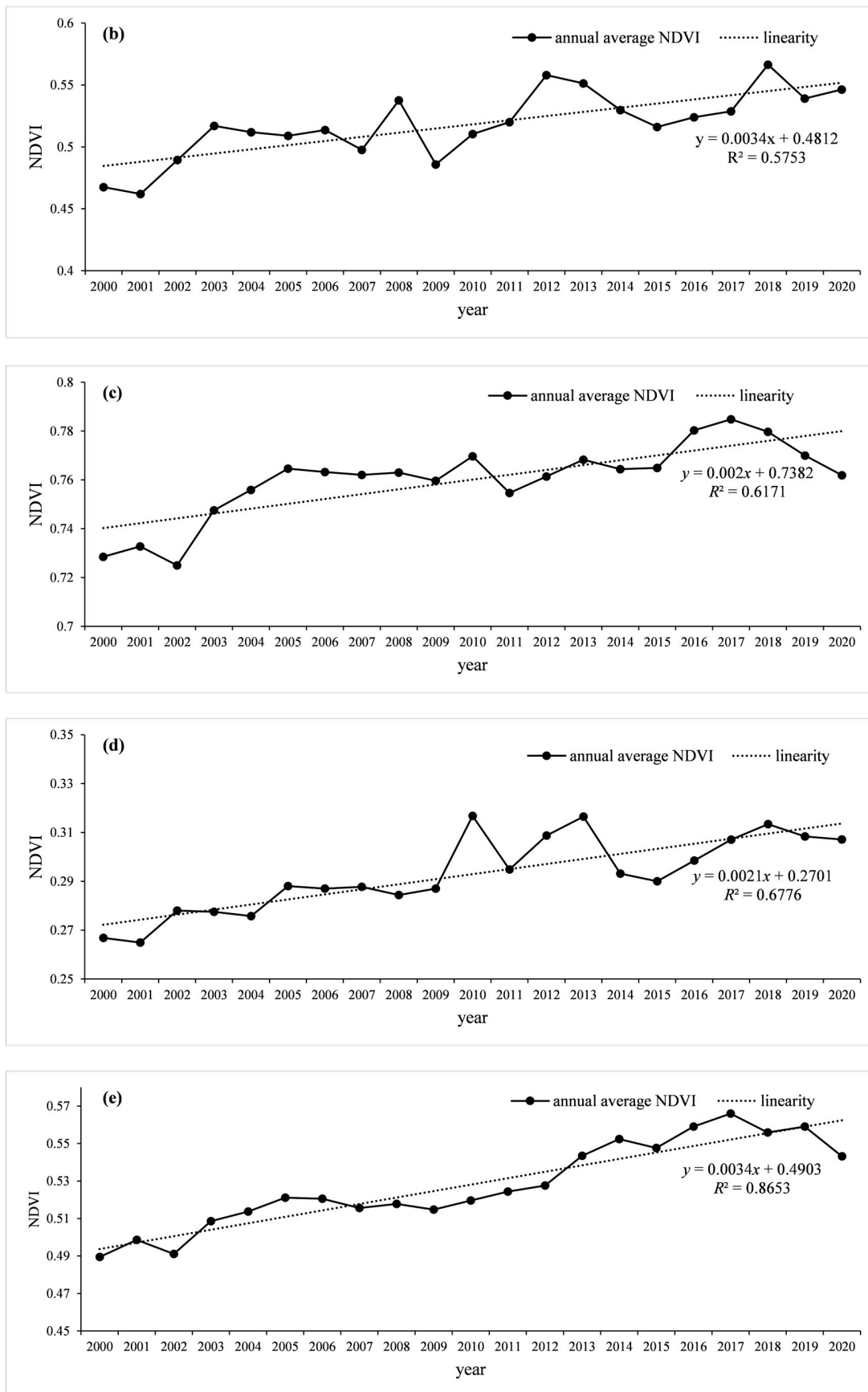


Figure 4. Cont.

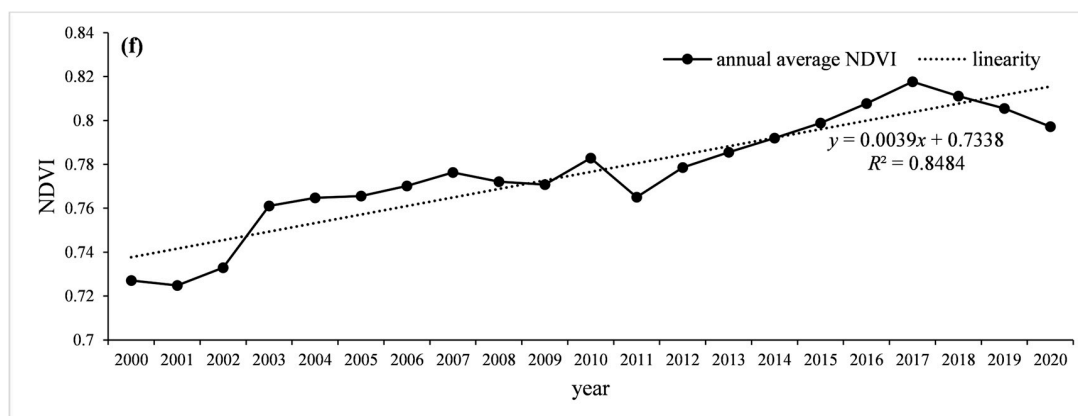


Figure 4. Interannual variation of NDVI in different regions: (a) Northeast China, (b) North China, (c) East China, (d) Northwest China, (e) Southwest China, (f) Central–South China.

As shown in Figure 4c, during 2000–2020, the NDVI fitting value of vegetation in East China increased by 0.002, the lowest increase among the six regions, and the overall trend showed an increasing trend of fluctuation. The goodness of fit R^2 was 0.6171, and the growth trend was more significant. The average annual maximum value appeared in 2017, which was 0.784, and the average annual minimum value appeared in 2002, which was 0.725. The highest increase was 0.01541 in 2015–2016, and the highest decrease was 0.015 in 2010–2011. Between 2005 and 2009, NDVI values remained relatively stable without significant fluctuations. During this period, the NDVI in East China peaked significantly at three specific times: in 2010, 2013, and 2017.

As shown in Figure 4d, during 2000–2020, the NDVI fitting value of vegetation in Northwest China increased by 0.0021, showing an increasing trend of fluctuation as a whole, and the goodness of fit R^2 was 0.6776, with a significant increase. The average annual maximum value appeared in 2018, which was 0.3134, and the average annual minimum value appeared in 2001, which was 0.264. The highest increase was 0.0298 in 2009–2010, and the highest decrease was 0.0234 in 2013–2014. From 2001 to 2008, over this extended period, the vegetation NDVI did not show significant changes, indicating a relatively stable trend.

As shown in Figure 4e, from 2000 to 2020, the NDVI fitting value of vegetation in Southwest China increased by 0.0034, showing a trend of increasing volatility as a whole, and the goodness of fit R^2 was 0.8653. Among the six regions, the goodness of fit is the highest, and the increase is the most significant. In 2017, the maximum value was 0.566, and the lowest value was 0.489 in 2000. The highest increase was 0.017 during 2002–2003, and the highest decrease was 0.0159 during 2019–2020. It can be observed that the annual average vegetation NDVI in the southwestern region shows an increasing trend, possibly related to the climate of the southwestern region, which is characterized by ample sunlight and abundant precipitation.

As shown in Figure 4f, during the period from 2000 to 2020, the NDVI fitting value of vegetation in the central and southern regions increased by 0.0039, with the highest increase in the fitting value. The overall trend showed an increasing trend of fluctuation, and the goodness of fit R^2 was 0.8484, with a significant increase. The highest increase was 0.0281 during 2002–2003, and the highest decrease was -0.0178 during 2010–2011. The trend indicates that despite fluctuations, vegetation cover in the Central–South region shows an overall growth trend.

Based on the analysis above, vegetation coverage levels in different regions can be categorized into three parts. The highest vegetation coverage is found in Northeast China, East China, and Central–South China, followed by North China and Southwest China. The northwest region exhibits the lowest vegetation coverage. Specifically, the northeast is known for its high-quality black soil conducive to agriculture. East China and Central–South China benefit from climates favorable for vegetation growth. The northwest, situated

deep inland with a continental climate and sparse precipitation, along with extensive desert areas, is less suitable for vegetation growth.

3.2.2. The Changes of Gravity Center in Different Partitions

To analyze and study the bias and variability in the distribution of the NDVI (normalized difference vegetation index) across different regions, a centroid model and standard deviation ellipse were employed. This analysis focused on the centroid distribution and migration trajectories of NDVI vegetation across six major regions from 2000 to 2020. The centroid model is a powerful tool in vegetation ecology, capable of describing and analyzing spatial and temporal variations and distributions of NDVI vegetation. This model, based on the centroid of vegetation the NDVI, allows for a more intuitive understanding and prediction of dynamic changes and ecological functions within vegetation communities. Additionally, this study calculated the distance (radial distance) and angle (angular displacement) from the centroid of NDVI mean values over 21 years, analyzing the specific distribution patterns of centroids in polar coordinates each year.

As shown in Figure 5(a1,a2) and Table 2, the gravity center of the vegetation NDVI in Northeast China was mainly distributed in Harbin, with a standard deviation ellipse angle of 13.08° . The distribution of the gravity center showed a northeast–southwest distribution pattern, indicating that the vegetation coverage in the northeast–southwest direction was higher. The standard deviation ellipse area was 37.61 km^2 , which was about twice that of Central–South China, indicating that the distribution of the gravity center was relatively concentrated, and the interannual spatial variation of vegetation coverage was small. Under the polar coordinates, among the four quadrants, the gravity centers were mostly distributed in the northwest quadrant, accounting for 38%, indicating that the vegetation coverage in the northwest was higher.

As shown in Figure 5(b1,b2) and Table 2, the vegetation NDVI gravity center in North China was mainly distributed in Xilinhot, and the standard deviation ellipse angle was 40.39° . The gravity center showed a distribution pattern in the northeast–southwest direction, indicating that the vegetation coverage in the northeast–southwest direction was higher. The standard deviation ellipse area was 34.51 km^2 , which was about twice that of Central–South China, indicating that the distribution of the gravity center was relatively concentrated, and the interannual spatial variation of vegetation coverage was small. Under polar coordinates, the gravity center in the southwest quadrant was the most distributed, accounting for 47%, indicating that the vegetation coverage in the southwest was high.

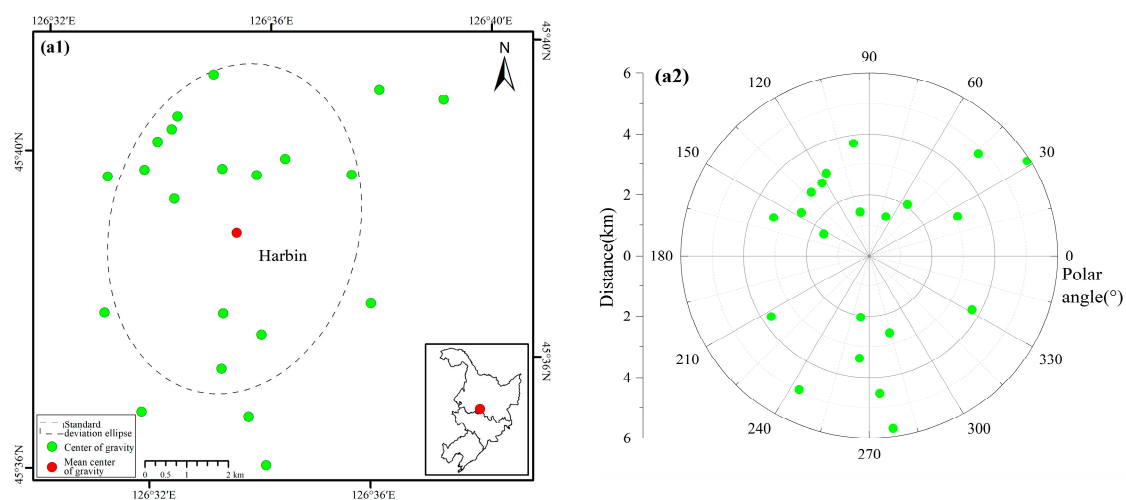


Figure 5. Cont.

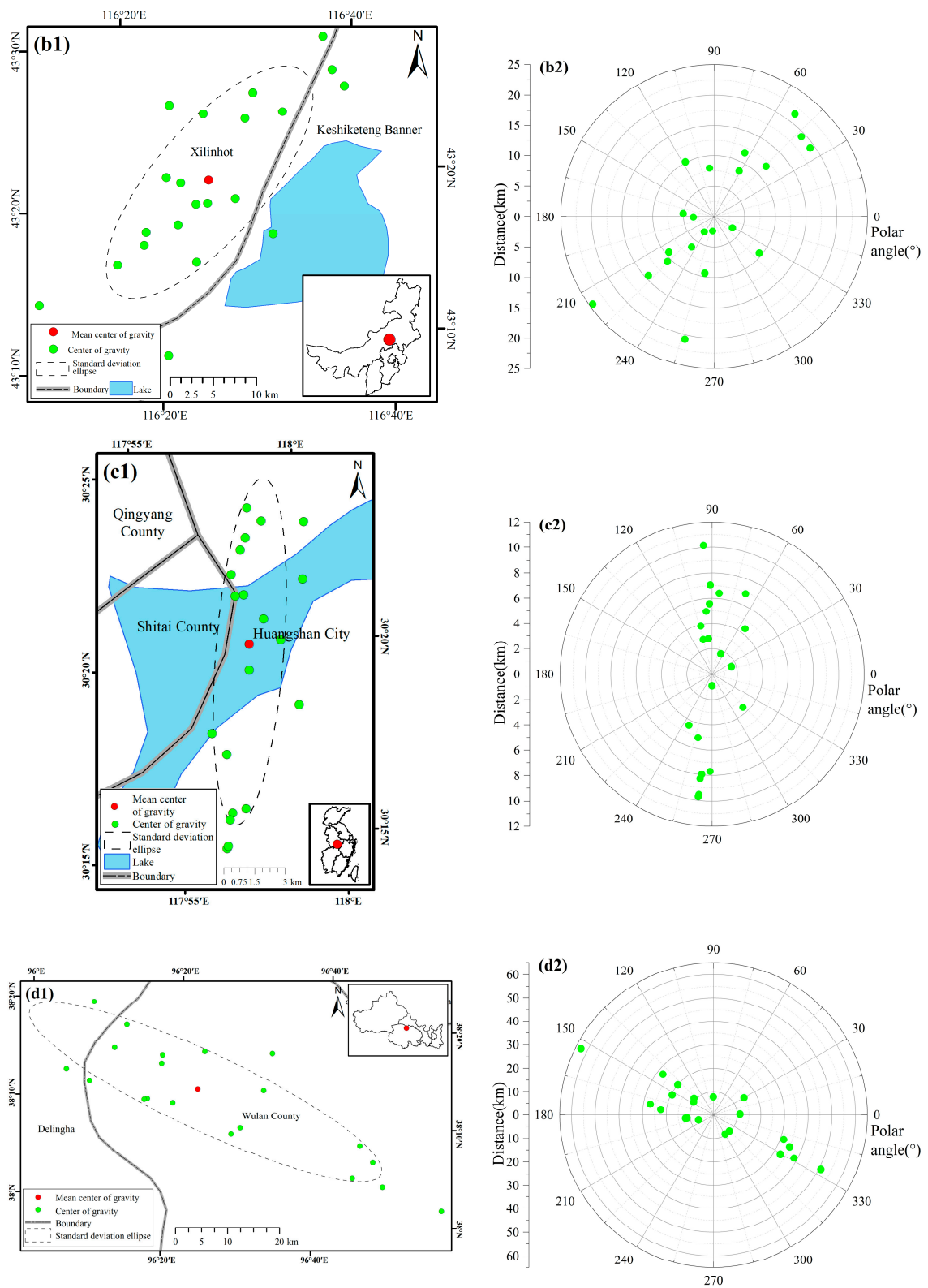


Figure 5. Cont.

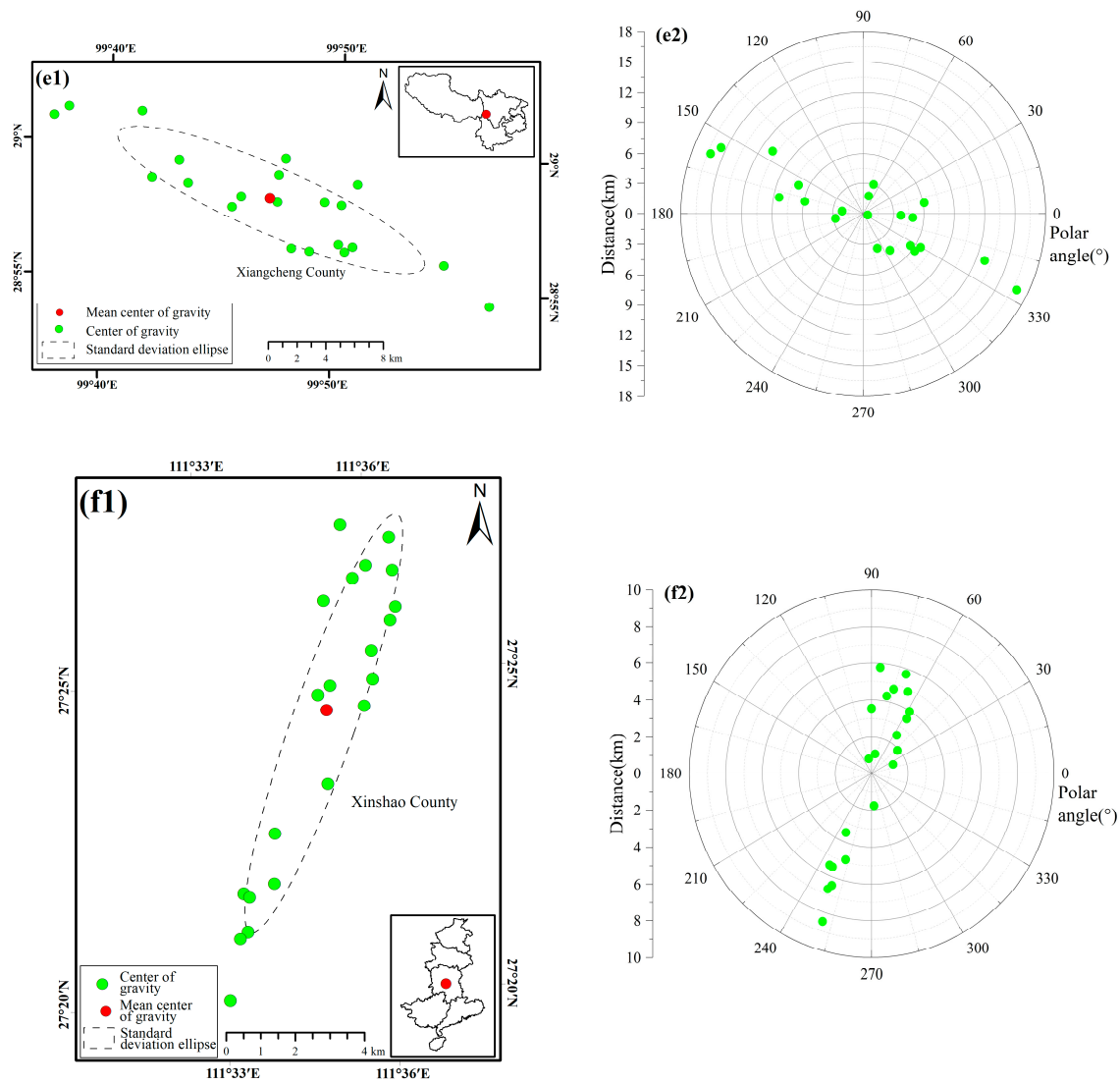


Figure 5. The gravity center of different partitions year by year: (a1) Northeast China (space); (a2) Northeast China (polar coordinates); (b1) North China (space); (b2) North China (polar coordinates); (c1) East China (space); (c2) East China (polar coordinates); (d1) Northwest China (space); (d2) Northwest China (polar coordinates); (e1) Southwest China (space); (e2) Southwest China (polar coordinates); (f1) Central–South China (space); (f2) Central–South China (polar coordinates).

Table 2. Different partition standard deviation ellipse parameters.

Standard Deviation Ellipse Parameters	Northeast China	North China	East China	Northwest China	Southwest China	Central–South China
Angle (°)	13.08	40.39	4.46	115.27	113.80	19.22
Standard deviation Along the <i>x</i> -axis (km)	2.986	6.508	1.661	3.731	11.61	0.923
Standard deviation Along the <i>y</i> -axis (km)	4.011	1.689	8.51	7.439	2.322	6.423
Elliptical area (km ²)	37.61	34.51	44.38	87.15	84.69	18.62

As shown in Figure 5(c1,c2) and Table 2, the gravity center in East China was mainly distributed in Huangshan City, with a standard deviation ellipse angle of 4.46°. The gravity center distribution generally showed a north–south distribution pattern, indicating that the north–south vegetation coverage was high. The standard deviation ellipse area was

44.38 km², indicating that the distribution of the gravity center was relatively concentrated, and the interannual spatial variation of vegetation coverage was small. Under the polar coordinates, the northern half (northeast quadrant and northwest quadrant) had the most gravity center distribution, accounting for 60%, indicating that the northern vegetation coverage was higher.

As shown in Figure 5(d1,d2) and Table 2, the gravity center in Northwest China was mainly distributed in Wulan County, with a standard deviation ellipse angle of 115.27°. The distribution of the gravity center showed a northwest–southeast distribution pattern, indicating that the vegetation coverage in the northwest–southeast direction was higher. The standard deviation ellipse area was 87.15 km², which was 4.7 times that of Central–South China, indicating that the gravity center distribution was the most discrete, and the interannual spatial variation of vegetation coverage was the largest. Under polar coordinates, the gravity center in the northwest and southeast quadrants accounted for about 40%, indicating that the vegetation coverage in the northwest and southeast directions was roughly the same.

As shown in Figure 5(e1,e2) and Table 2, the gravity center of the southwest region was mainly distributed in Xiangcheng County, with a standard deviation ellipse angle of 113.8°. The distribution of the gravity center showed a northwest–southeast distribution pattern, indicating that the vegetation coverage in the northwest–southeast direction was higher. The standard deviation ellipse area was 84.69 km², which was about 4.5 times that of Central–South China, indicating that the distribution of the gravity center was relatively discrete, and the interannual spatial variation of vegetation coverage was large. Under the polar coordinates, the distribution of the gravity center in the southeast quadrant was relatively high, with about 42%, indicating that the vegetation coverage in the southeast was high.

As shown in Figure 5(f1,f2) and Table 2, the gravity center in Central–South China was mainly distributed in Xinshao County, with a standard deviation ellipse angle of 19.22°. The center of gravity showed a northeast–southwest distribution pattern, indicating that the vegetation coverage in the northeast–southwest direction was higher. The standard deviation ellipse area was 18.62 km², and the standard deviation ellipse area was the smallest, indicating that the center of gravity was the most concentrated and the interannual spatial variation of vegetation coverage was the smallest. Under the polar coordinates, the gravity center in the northeast quadrant was relatively high, about 62%, indicating that the vegetation coverage in the northeast was high.

The change law of vegetation coverage migration in different regions was further explored using the center of gravity migration trajectory. As shown in the figure, the center of gravity migration was analyzed on a 4-year time scale.

As shown in Figure 6a, the gravity center of Northeast China showed a mitigation trend of northwest–southwest–northwest from 2000 to 2020. During 2004–2007→2008–2011, the migration distance to the southwest was the farthest, which was 2.34 km, indicating that the increment and growth rate of vegetation coverage in the southwest during 2008–2011 were much larger than those in other time periods. The gravity center of vegetation coverage in Northeast China showed a trend of mitigating to the northwest, indicating that the increase and growth rate of vegetation coverage in the northwest direction was higher.

As shown in Figure 6b, the gravity center of North China showed a changing trend of southeast–southwest–southeast from 2000 to 2020. During 2012–2015→2016–2020, the migration distance to the southeast was the farthest, which was 6.04 km, indicating that the increase and growth rate of vegetation coverage in the southeast direction during 2016–2020 were much larger than those in other time periods. The gravity center of vegetation coverage in North China showed a trend of mitigating to the southwest, indicating that the increase and growth rate of vegetation coverage in the southwest direction was higher.

As shown in Figure 6c, the gravity center in East China showed a mitigation trend of northwest–southwest from 2000 to 2020. During 2008–2011→2012–2015, the migration distance to the southwest was the farthest, at 6.00 km, indicating that the increment and

growth rate of vegetation coverage in the southwest during 2012–2015 were much larger than those in other time periods. The gravity center of vegetation coverage in East China showed a trend of mitigating to the southwest, indicating that the increase and growth rate of vegetation coverage in the southwest was higher.

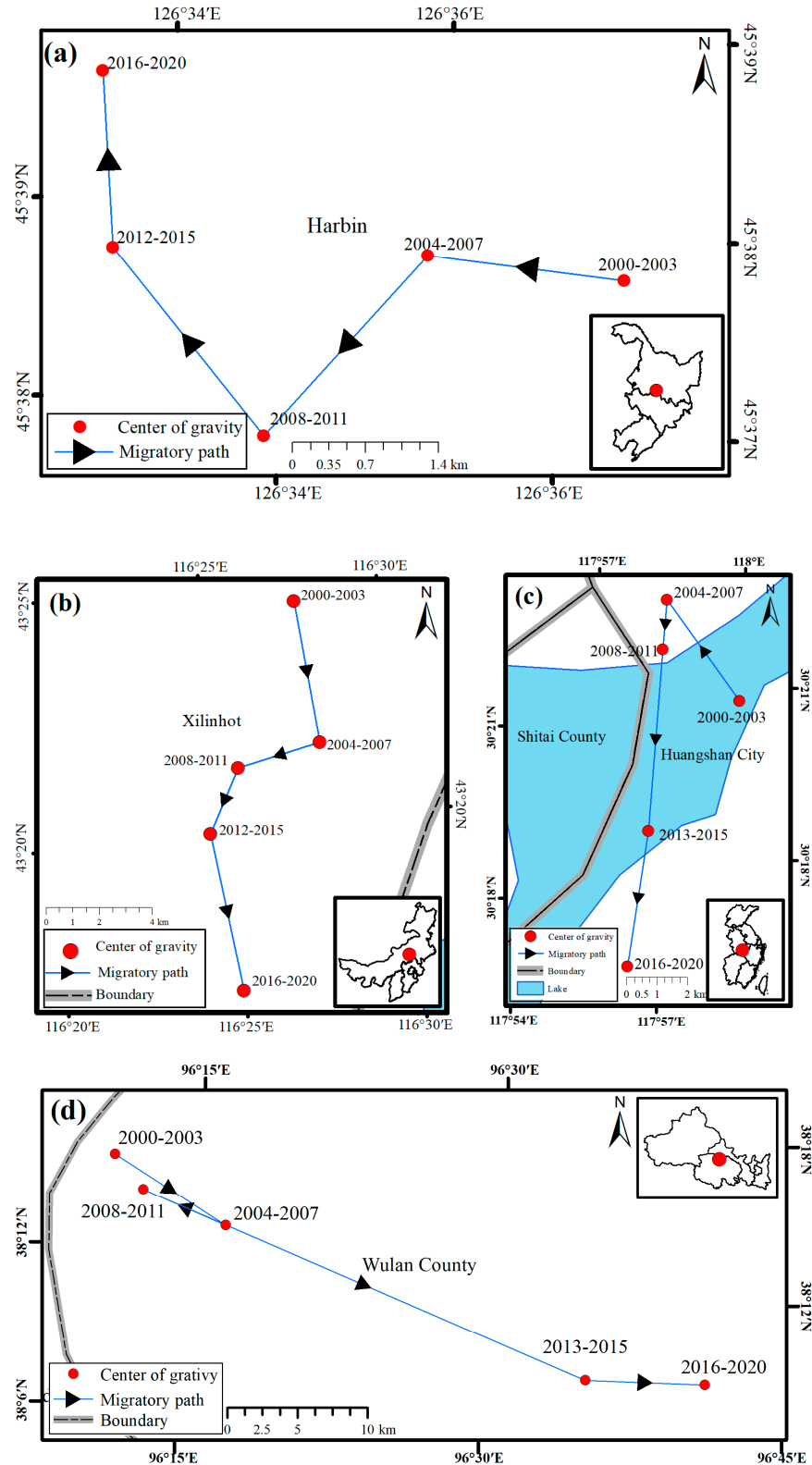


Figure 6. Cont.

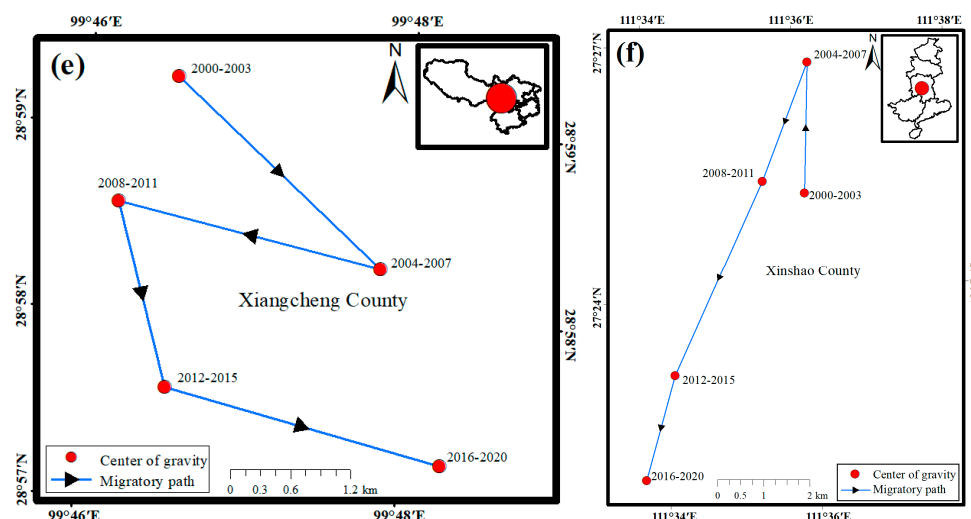


Figure 6. Different partition migration routes: (a) Northeast China; (b) North China; (c) East China; (d) Northwest China; (e) Southwest China; (f) Central–South China.

As shown in Figure 6d, the gravity center of Northwest China showed a mitigation trend of southeast–northwest–southeast from 2000 to 2020. During 2008–2011→2012–2015, the migration distance to the southeast was the farthest, 34.31 km, indicating that the increase and growth rate of vegetation coverage in the southeast during 2012–2015 was much greater than other time periods. The gravity center of vegetation coverage in Northwest China showed a trend of mitigating to the southeast, indicating that the increase and growth rate of vegetation coverage was higher.

As shown in Figure 6e, the gravity center of Southwest China showed a mitigation trend of southeast–northwest–southeast between 2000 and 2020. During 2012–2015→2016–2020, the migration distance to the southeast was the farthest, at 2.85 km, indicating that the increase and growth rate of vegetation coverage in the southeast during 2016–2020 was much greater than other time periods. The gravity center of vegetation coverage in Southwest China showed a trend of mitigating to the southeast, indicating that the increase and growth rate of vegetation coverage in the southeast was higher.

As shown in Figure 6f, the gravity center of Central–South China showed a mitigation trend of northwest–southwest from 2000 to 2020. During 2008–2011→2012–2015, the migration distance to the southwest was the farthest, 4.64 km, indicating that the increment and growth rate of vegetation coverage in the southwest during 2012–2015 were much larger than those in other time periods. The gravity center of vegetation coverage in Central–South China showed a trend of mitigating to the southwest, indicating that the increase and growth rate of vegetation coverage in the southwest was higher.

3.2.3. Area Changes of Different Grades

In order to analyze the area change of vegetation coverage grade in different periods, the study period was divided into two historical periods, namely, 2000–2010 and 2011–2020, as shown in Figure 6.

As shown in Figure 7a, during 2000–2010, the area of vegetation coverage grade change from medium–high vegetation coverage to high vegetation coverage accounted for the highest proportion, 54%, mainly distributed in South China, such as Anhui Province, Hunan Province, Guizhou Province, and other regions. It was also distributed at the junction of the Inner Mongolia Plateau, Daxing’an Mountains, and Northeast Plain in Northeast China, followed by the change from medium vegetation coverage to medium–high vegetation coverage, accounting for about 14%, mainly concentrated at the junction of the second and third steps. The area with increased vegetation coverage grade was 92%, and the area with decreased vegetation coverage grade was 8%, indicating that the vegetation coverage grade showed an increasing trend from 2000 to 2010.

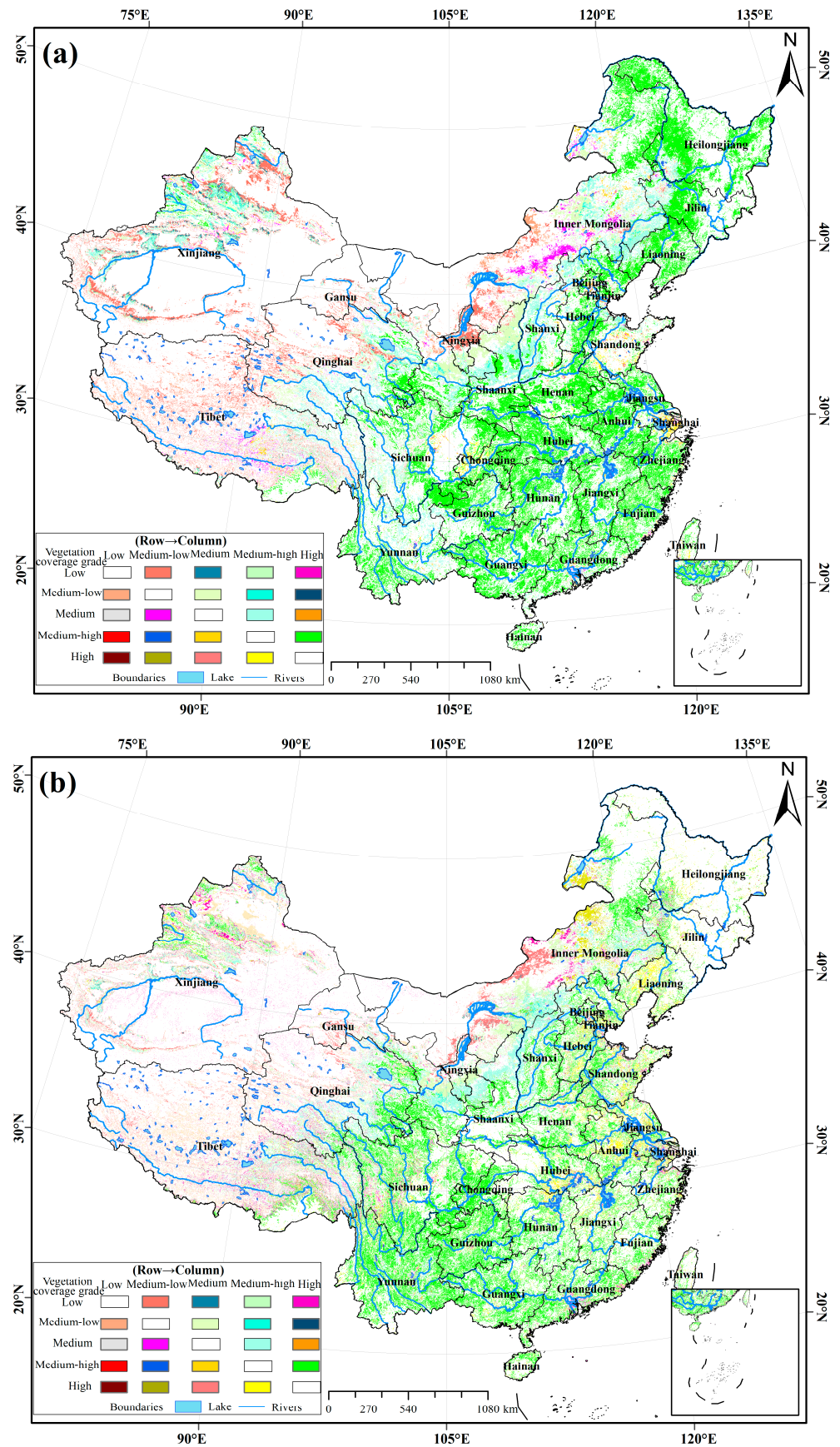


Figure 7. Changes of NDVI transfer at different grades in different time periods: (a) 2000–2010 and (b) 2011–2020.

As shown in Figure 7b, during 2011–2020, the area of vegetation coverage grade change from medium–high vegetation coverage to high vegetation coverage accounted for the highest proportion, 43%, mainly distributed in southern China, such as Guizhou Province and Yunnan Province. The conversion area from medium vegetation coverage to medium–high vegetation coverage was the second largest, with an area ratio of about 11%, mainly distributed at the junction of the Inner Mongolia Plateau and the Loess Plateau. The area with increased vegetation coverage grade accounted for 71%, while that with decreased vegetation coverage grade accounted for 29%, indicating that the vegetation coverage grade showed an increasing trend from 2011 to 2020.

3.3. Lag Time Analysis

Because the growth of vegetation was significantly affected by temperature and precipitation, it took a certain amount of time for temperature and precipitation to reflect the growth of vegetation; that is, vegetation experienced a certain time lag regarding the relationship between temperature and precipitation. At the same time, different geographical locations and different vegetation types had certain impacts on the hysteresis. To explore the lagged effects of the monthly vegetation NDVI on temperature and precipitation across different regions of China and to analyze how vegetation growth is significantly influenced by precipitation, meteorological stations were selected for correlation coefficient analysis. For precipitation, the lagged response depends on the time it takes for moisture to be absorbed by vegetation roots and then for vegetation growth to reflect in its normalized difference vegetation index (NDVI) values. This temporal delay manifests as a lagged responsiveness of the NDVI to precipitation. According to Table 3, the Chinese vegetation NDVI is primarily influenced significantly by precipitation from 1–3 months (i.e., the sum of precipitation from the previous months to three months ago), with a correlation coefficient of 0.673. Following closely behind is precipitation from 1–2 months, which also has a high correlation coefficient of 0.815. Conversely, precipitation from the previous 3 months has a relatively minor impact on the NDVI in the current months, with a correlation coefficient of only 0.158. As shown in Figure 7, the correlation coefficient between the vegetation NDVI and temperature and precipitation in different periods was obtained.

Table 3. Analysis of correlation coefficients between NDVI and lagged months of precipitation.

RAIN/NDVI	Current Months	Previous Months	Two Months Ago	Three Months Ago	One to Two Months	One to Three Months
correlation coefficient	0.533	0.580	0.434	0.158	0.651	0.673

As shown in Figure 8a, the time lag of the vegetation NDVI and precipitation was generally 1–2 months and 1–3 months. Zones with a time lag of 1–2 months were mainly distributed at the junction of the second and third steps, the East China Plain, and the Qinghai–Tibet Plateau. Zones with a time lag of 1–3 months were mainly distributed in the Northeast Plain, the middle and lower reaches of the Yangtze River Plain, and other regions. As shown in Figure 8b, the time lag of the vegetation NDVI and temperature lag were generally the current months, 1–3 months, and 1–2 months. Among them, the zone with the time lag of current months was mainly distributed in the plain area of East China, while that 1–3 was mainly distributed in the junction of the second and third levels of succession, the coastal area of southern China, and other areas. In addition, the zone time lag of 1–2 months was mainly distributed in the hilly areas of Liaodong, the Qinghai–Tibet Plateau, the southeast hills, and other areas.

Based on the above analysis, the time lag for cultural vegetation, shrubs, and precipitation is generally 1–3 months, while the time lag for meadows, shrubs, and precipitation is generally 1–2 months. The time lag for artificial vegetation, coniferous forests, and air temperature is generally the same month, and the time lag for broad-leaved forests and air temperature is generally 1–2 months.

As shown in Figure 9(a1), the coniferous forest vegetation in Northeast China was most affected by precipitation over 1–2 months, with a correlation coefficient of 0.82, and the vegetation types such as cultivated vegetation were most affected by precipitation over 1–3 months. As shown in Figure 9(a2), different vegetation types in Northeast China were most affected by temperature over 1–2 months, followed by the current monthly temperature on the coniferous and broad-leaved forest, with a correlation coefficient of 0.92, and the temperature over 1–3 months had the second greatest impact on other vegetation types.

As shown in Figure 9(b1), cultural vegetation, coniferous forests, and herbosa in East China were most affected by the current monthly precipitation, with correlation coefficients of 0.73, 0.72, and 0.82, respectively, followed by 1–2 months, with correlation coefficients of 0.72, 0.72, and 0.81, respectively. Broad-leaved forests were most affected by precipitation of 1–3 months, with a correlation coefficient of 0.60, followed by that of one month, with a correlation coefficient of 0.59. Shrubs were most affected by precipitation of 1–2 months, with a correlation coefficient of 0.72, followed by that of 1–3 months, with a correlation coefficient of 0.81. As shown in Figure 9(b2), shrubs and broad-leaved forests in East China were most affected by temperature over two months, with the correlation coefficients of 0.42 and 0.34, respectively. Other vegetation types were most affected by temperature from January to February, and the correlation coefficients were 0.347.

As shown in Figure 9(c1), the different vegetation types in Northwest China were most affected by the precipitation over the 1–2 months, and the correlation coefficients for grasslands, broad-leaved forests, and shrubs were 0.78, 0.74, and 0.76, respectively. They were all affected by precipitation over 1–3 months, and the correlation coefficients for grasslands, coniferous forests, and meadows were 0.78, 0.73, and 0.70, respectively. As shown in Figure 9(c2), different vegetation types in Northwest China were most affected by temperature over 1–2 months, among which the correlation coefficients for swamps, broad-leaved forests, and coniferous forests were 0.96, 0.93, and 0.89, respectively. The influence of the current months on coniferous forests, swamps, and grass was second, and the correlation coefficients were 0.86, 0.95, and 0.86, respectively.

As shown in Figure 9(d1), broad-leaved forests, meadows, and grassland in North China were most affected by the precipitation one month ago, and the correlation coefficients were 0.85, 0.86 and 0.74, respectively. Bog, bush-wood, and herbosa were most affected by precipitation in the 1–2 months, and the correlation coefficients were 0.92, 0.86 and 0.83, respectively. Cultural vegetation and coniferous forests were most affected by precipitation in the 1–3 months, and the correlation coefficients were 0.86 and 0.89, respectively. As shown in Figure 9(d2), coniferous forest, broad-leaved forest and grassland in North China were most affected by the temperature in the 1–3 months, and the correlation coefficients were 0.82, 0.77 and 0.81, respectively. Other vegetation types were most affected by temperature from January to February.

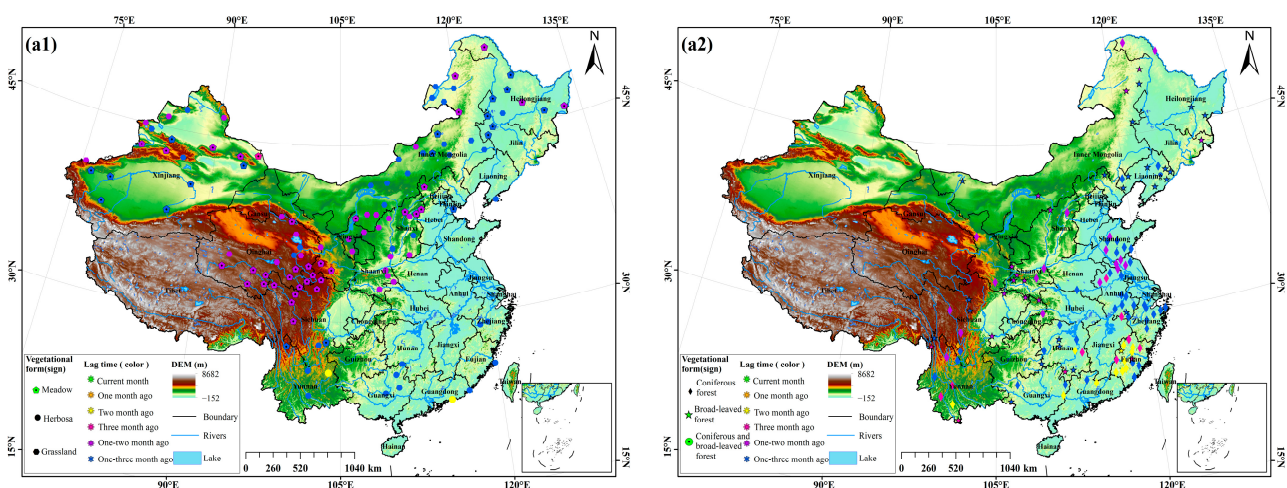


Figure 8. Cont.

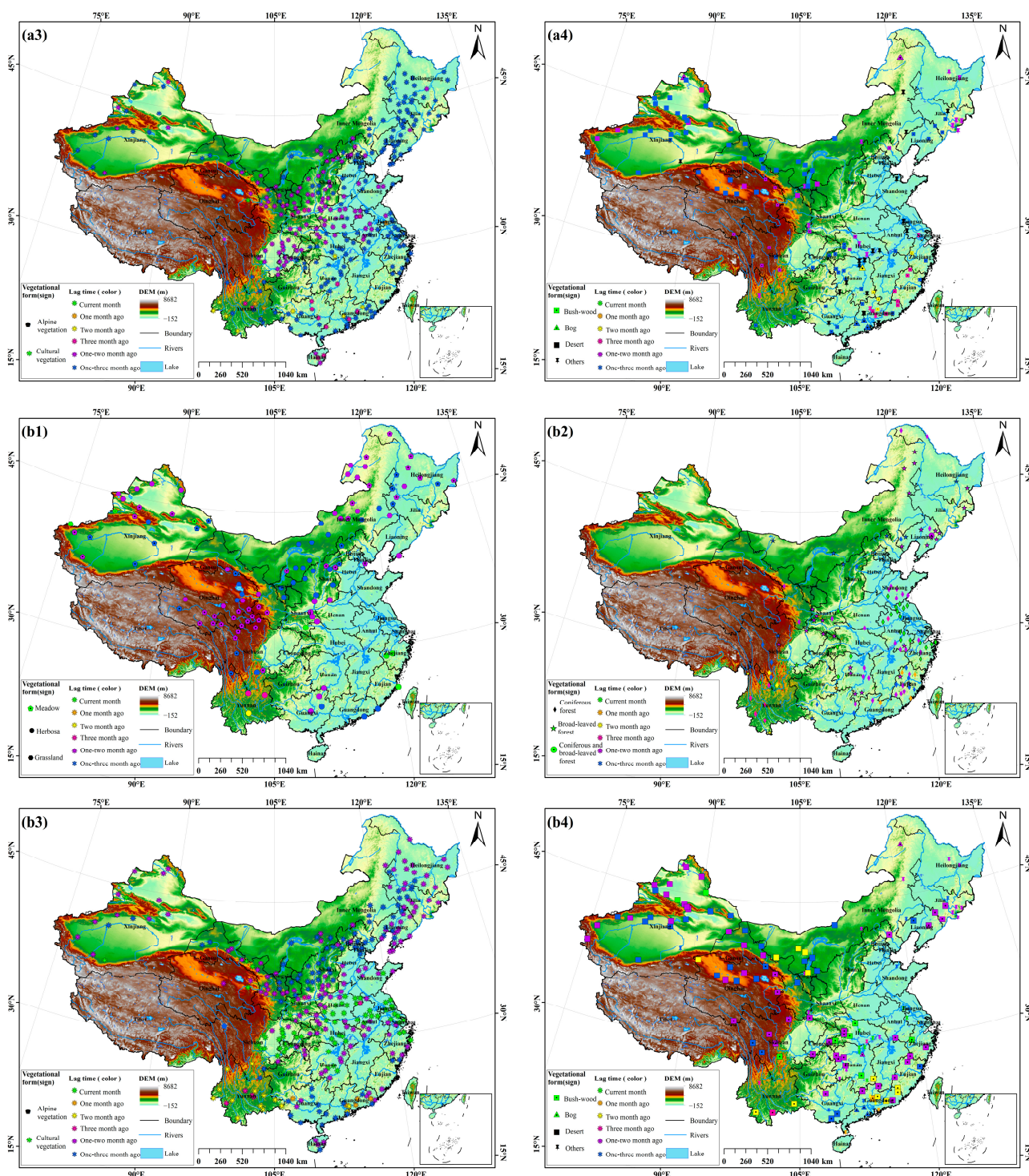


Figure 8. Spatial distribution of lag of time for different vegetation types. (a1) Precipitation (meadow; herbosa; grassland); (a2) precipitation (coniferous forest; broad-leaved forest; coniferous and broad-leaved forest); (a3) precipitation (alpine vegetation; cultural vegetation); (a4) precipitation (bush-wood; bog; desert; others); (b1) temperature (meadow; herbosa; grassland); (b2) temperature (coniferous forest; broad-leaved forest; coniferous and broad-leaved forest); (b3) temperature (alpine vegetation; cultural vegetation); (b4) temperature (bush-wood; bog; desert; others).

As shown in Figure 9(e), meadows and alpine vegetation in Southwest China were most affected by precipitation over 1–2 months, with correlation coefficients of 0.83 and 0.91, respectively. Other vegetation types were most affected by precipitation over the

1–3 months. As shown in Figure 9(e2), shrubs in Southwest China were most affected by temperature over 1–3 months, and the correlation coefficient was 0.67. Coniferous forests and herbosa were most affected by temperature over two months, and the correlation coefficients were 0.47 and 0.55, respectively. Other vegetation types were most affected by temperature over 1–2 months.

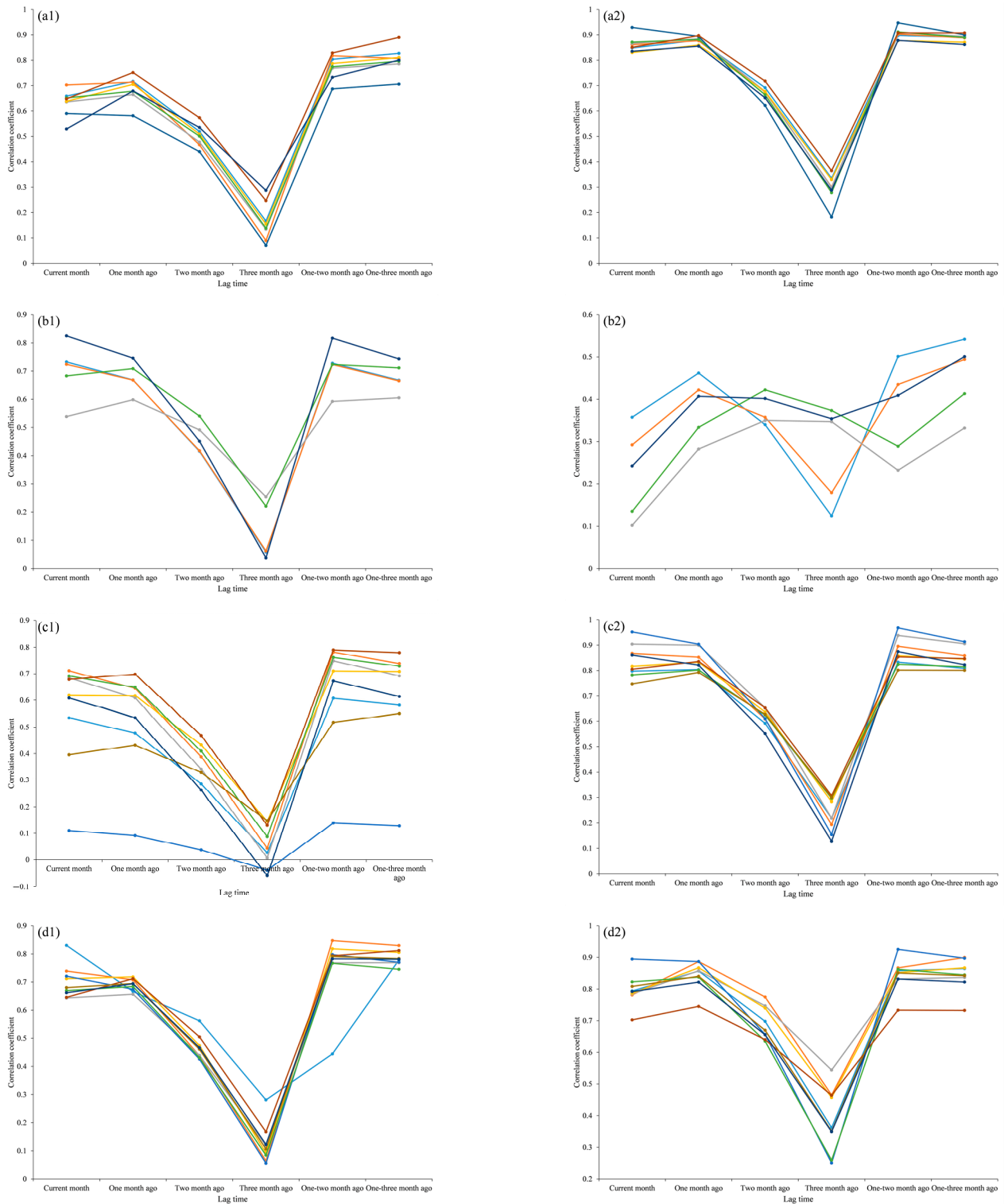


Figure 9. Cont.

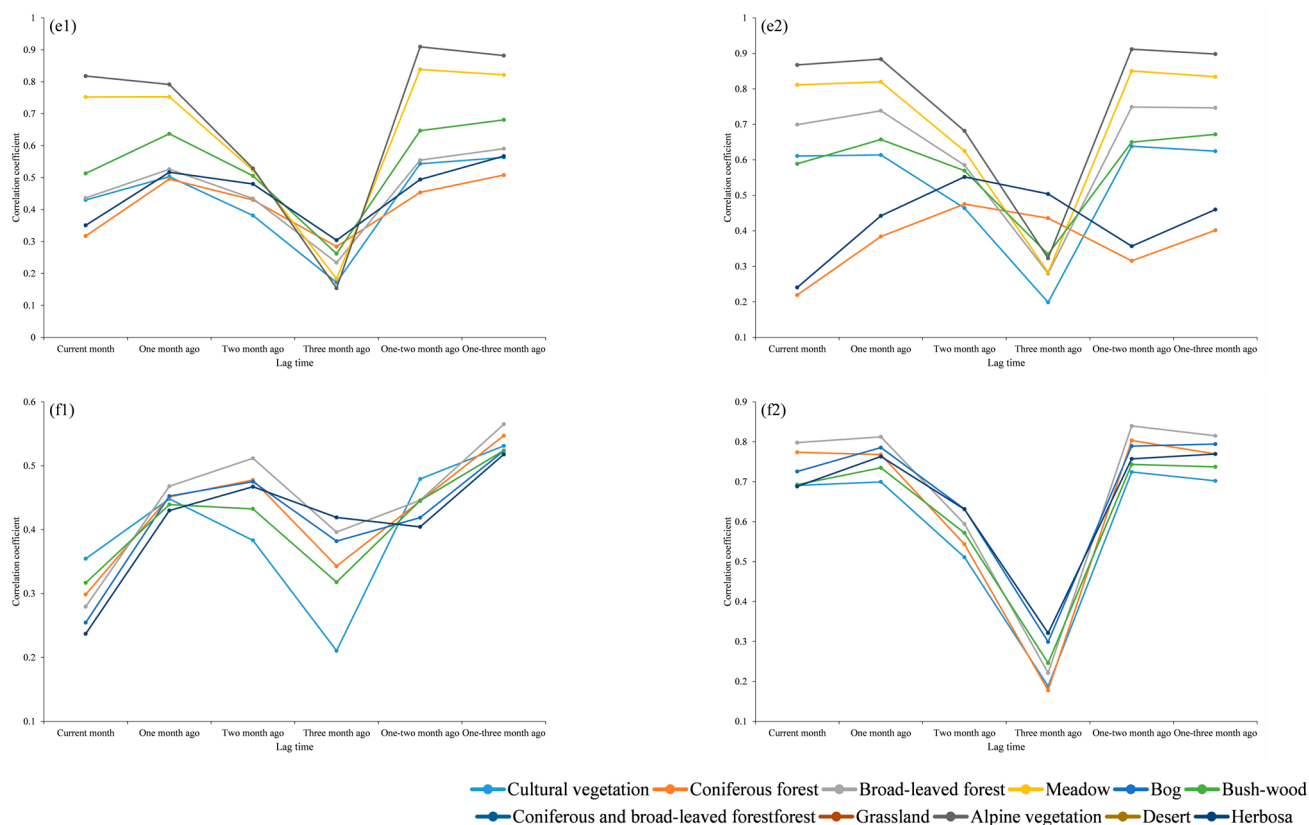


Figure 9. Lag time in different regions: (a1) Northeast China (precipitation); (a2) Northeast China (temperature); (b1) East China (precipitation); (b2) East China (temperature); (c1) Northwest China (precipitation); (c2) Northwest China (temperature); (d1) North China (precipitation); (d2) North China (temperature); (e1) Southwest China (precipitation); (e2) Southwest China (temperature); (f1) Central–South China (precipitation); (f2) Central–South China (temperature).

As shown in Figure 9(f1), different vegetation types in Central South China were most affected by precipitation over the 1–3 months. The correlation coefficients for broad-leaved forests, coniferous forests, and cultural vegetation were 0.56, 0.54, and 0.53, respectively. Precipitation over 1–2 months had the second greatest impact on cultural vegetation and shrubs, and the correlation coefficients were 0.479 and 0.445, respectively. Precipitation over two months had the second greatest impact on other vegetation types.

3.4. Dominant Factors of Vegetation Change in Different Historical Periods and Different Sub-Regions

3.4.1. Correlations with Typical Climate Factors

In order to analyze the correlation between the vegetation NDVI and climatic factors from 2000 to 2020, three climatic factors, temperature, precipitation, and accumulated temperature, were selected in this study. The second-order partial correlation coefficient was used to explore the correlation between the vegetation NDVI and climatic factors, and the significance test was carried out, as shown in Figure 10.

As shown in Figure 10(a1,a2), the partial correlation coefficient between the vegetation NDVI and temperature ranged from -0.94 to 0.95 . It was mainly distributed in the southern Qinghai–Tibet Plateau, Wuyi Mountains, Yunnan–Guizhou Plateau, and other regions. The area with extremely significant positive correlation accounted for 4.2%, mainly distributed in the Xiaoxing’an Mountains, the southeastern hilly areas, and the surrounding areas with extremely significant positive correlation. The areas with significant negative correlation accounted for 4.2%, mainly distributed in the eastern part of the Inner Mongolia Plateau and Qaidam Basin. As shown in Figure 10(b1,b2), the partial correlation coefficient between the vegetation NDVI and precipitation ranged from -0.89 to 0.96 . The area of significant

positive correlation was about 10%, mainly distributed in the surrounding areas of very significant positive correlation. The area of significant negative correlation was 1.9%, mainly distributed in the Turpan Basin, western Inner Mongolia Plateau, and other regions. As shown in Figure 10(c1,c2), the partial correlation coefficient between the NDVI and accumulated temperature ranged from -0.97 to 0.93 , and the area of very significant positive correlation was 3.9%, which was mainly distributed in Gansu, the Tianshan Mountains, the Ningxia Hui Autonomous Region, and Shaanxi Province. The area of significant positive correlation was 2.3%, which was mainly distributed in the surrounding area of very significant positive correlation. The area of significant negative correlation was 2.9%, mainly distributed in Guizhou Province and other regions.

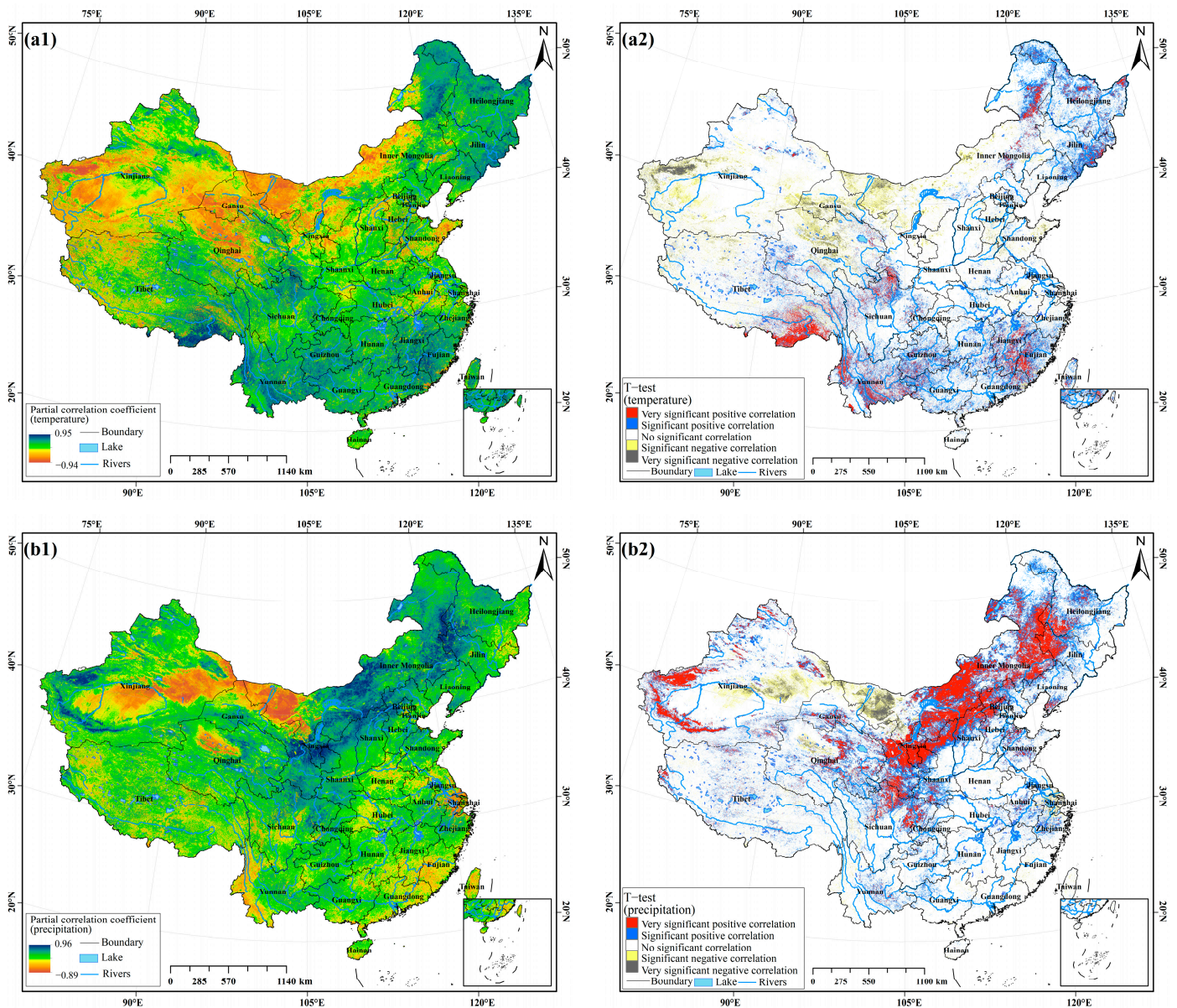


Figure 10. Cont.

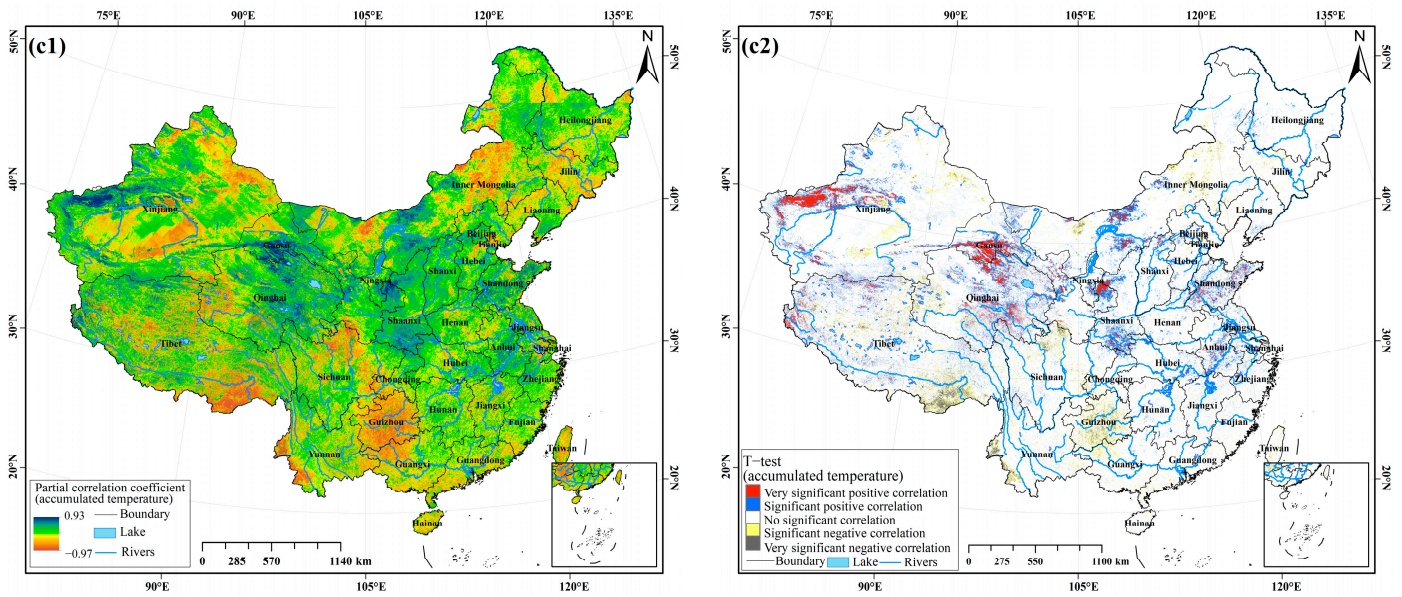


Figure 10. Partial correlation coefficient and significance test: (a1) temperature partial correlation coefficient; (a2) temperature significance test; (b1) precipitation partial correlation coefficient; (b2) precipitation significance test; (c1) accumulated temperature partial correlation coefficient; (c2) accumulated temperature significance test.

3.4.2. Dominant Factor Analysis of Different Partitions

(1) Single factor

In different regions and different historical periods, the driving factors of the NDVI are effectively distinguished by geographic detectors. In this study, climate factors (sunshine, accumulated temperature, temperature, and precipitation), human activity factors (GDP and population density), and terrain factors (altitude, slope, and land use) were selected to analyze the driving mechanism of the vegetation NDVI. The dominant single factors of each of the six major zones are shown in Figure 11.

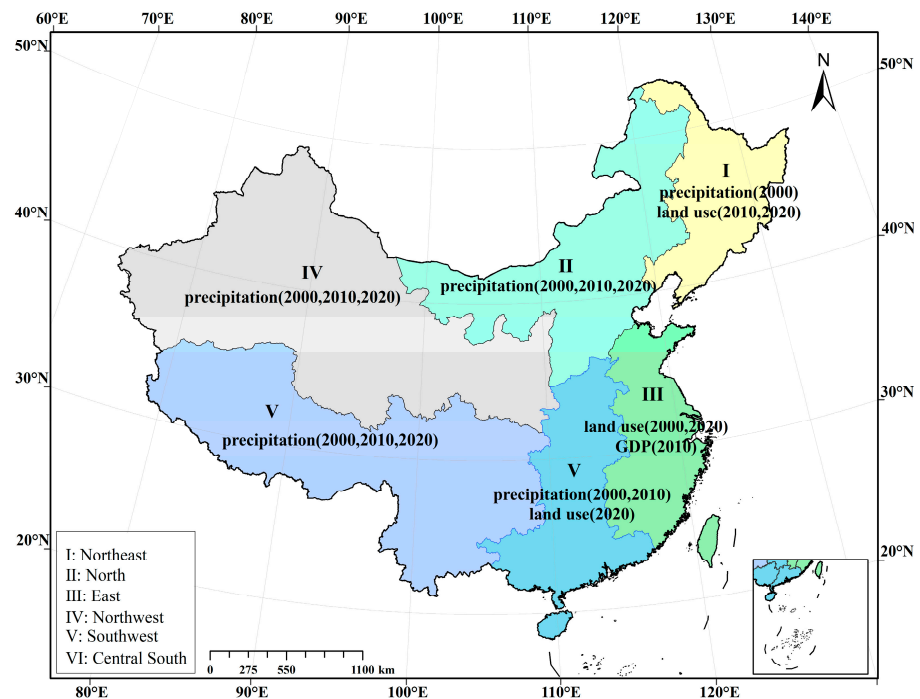


Figure 11. The distribution map of NDVI dominant factors in China’s six major zones.

As shown in Figure 12a, in 2000, 2010, and 2020, the factors with the strongest impact on the vegetation NDVI in Northeast China were precipitation and land use, with q-values of 0.47, 0.52, and 0.32, respectively. In 2010–2020, land use had a greater impact on vegetation growth, which might be related to the gradual increase in the local urbanization level, which, in turn, affected vegetation growth. GDP and population density had the weakest influences on the vegetation NDVI, and the q-value was less than 0.1, indicating that local human activities had little effect on vegetation growth.

As shown in Figure 12b, in 2000, 2010, and 2020, the factor that had the strongest impact on the vegetation NDVI in North China was precipitation, and the q-values were 0.71, 0.80, and 0.74, respectively, indicating that precipitation had the greatest impact on vegetation growth in North China. Population density had the weakest impact on the vegetation NDVI in North China, and the q-value was less than 0.1, which might be related to the sparse population in the Inner Mongolia Plateau and other regions.

As shown in Figure 12c, in 2000, 2010, and 2020, the factors that had the strongest impact on the vegetation NDVI in East China were land use, GDP, and land use, respectively, with q-values of 0.42, 0.43, and 0.58. The factors that had the weakest impact on the vegetation NDVI were precipitation, altitude, and temperature, respectively, with q-values of 0.1, 0.12, and 0.13.

As shown in Figure 12d, in 2000, 2010, and 2020, the factor that had the strongest impact on the vegetation NDVI in Northwest China was precipitation, with q-values of 0.65, 0.65, and 0.59, respectively. Accumulated temperature and population density had the weakest influence on the vegetation NDVI, and the q-value was less than 0.1.

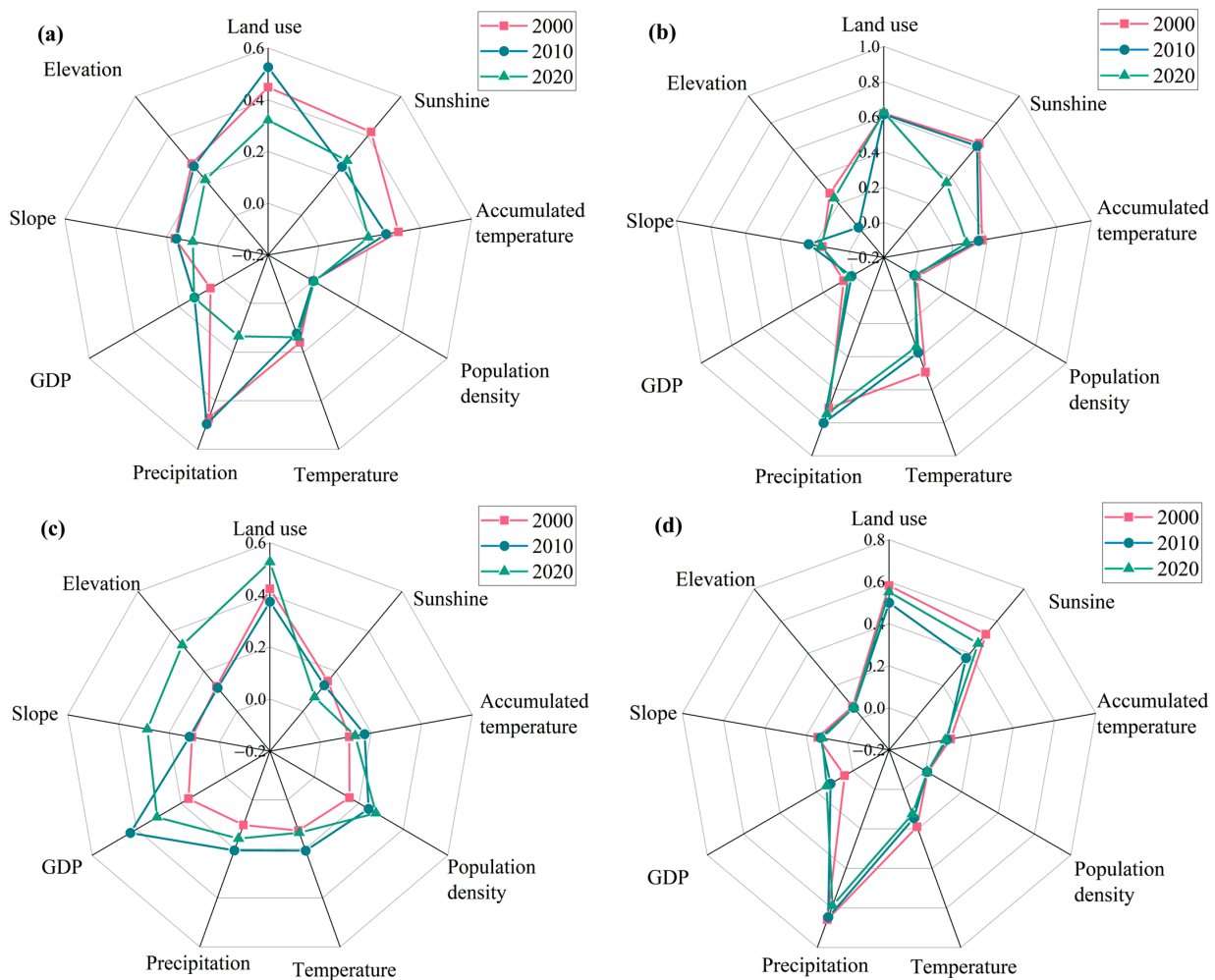


Figure 12. Cont.

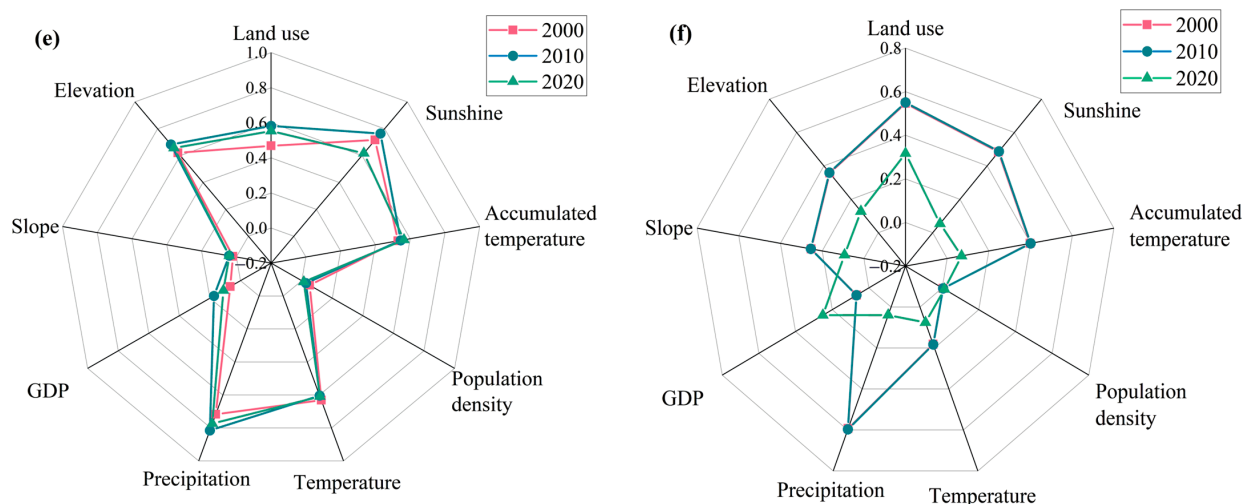


Figure 12. Single factors: (a) Northeast China; (b) North China; (c) East China; (d) Northwest China; (e) Southwest China; (f) Central–South China.

As shown in Figure 12e, in 2000, 2010, and 2020, the factor that had the strongest impact on the vegetation NDVI in Southwest China was precipitation, with q-values of 0.71, 0.81, and 0.77, respectively, followed by sunshine and altitude, with q-values of 0.71, 0.76 and 0.65, respectively.

As shown in Figure 12f, in 2000, 2010, and 2020, the factors that had the strongest impact on the vegetation NDVI in Central South China were precipitation and land use, respectively, with q-values of 0.59, 0.59, and 0.32. The precipitation in Central–South China was more conducive to the growth of vegetation. The factor with the weakest impact on the vegetation NDVI was population density, and the q-values were 0.005, 0.005, and 0.012, respectively.

(2) Interaction factor

The interaction between different factors has different effects on the vegetation NDVI, and the interaction between different regions is different. Therefore, the interaction factors affecting vegetation NDVI change were analyzed by a geographic detector.

As shown in Figure 13(a1–a3), the interaction between most factors in Northeast China was nonlinearly enhanced. The dominant interaction factors in 2000, 2010, and 2020 were accumulated temperature \cap sunshine, precipitation \cap land use, and accumulated temperature \cap land use, respectively, with q-values of 0.752, 0.87, and 0.52. Among them, land uses had strong interaction effects with other factors on the vegetation NDVI in 2010 and 2020, indicating that with the improvement of the urbanization level, land use change became an important factor affecting vegetation cover. As shown in Figure 13(b1–b3), the interaction between most factors in North China was enhanced by two factors. The strongest interaction factors in 2000, 2010, and 2020 were precipitation \cap temperature, precipitation \cap land use, and precipitation \cap land use, respectively, with q-values of 0.842, 0.855, and 0.828. In 2010 and 2020, the dominant interactive factor was precipitation \cap land use, indicating that precipitation \cap land use had the strongest influence on the vegetation NDVI in North China. As shown in Figure 13(c1–c3), the interaction between most factors in East China was nonlinearly enhanced. The strongest interaction factors in 2000, 2010, and 2020 were sunshine \cap land use, temperature \cap land use, and precipitation \cap land use, respectively, with q-values of 0.640, 0.626, and 0.640. The urbanization level in East China was higher, which had a greater impact on the vegetation NDVI. The other dominant factors of interaction were climate factors, indicating that with the climate change in North China, climate played a dominant role in vegetation growth. As shown in Figure 13(d1–d3), the interaction between most factors in Northwest China was enhanced by two factors. The strongest interaction factor in 2000, 2010, and 2020 was precipitation \cap land use, with q-values of 0.814, 0.740, and 0.753, respectively, indicating that precipitation and land use

had the strongest impacts on the vegetation NDVI in Northwest China. As shown in Figure 13(e1–e3), the interaction between most factors in Southwest China was a two-factor enhancement. The strongest interaction factors in 2000, 2010, and 2020 were sunshine \cap land use, precipitation \cap land use, and precipitation \cap land use, respectively, with q-values of 0.785, 0.854, and 0.806. As shown in Figure 13(f1–f3), the interaction between most factors in Central–South China was a two-factor enhancement. The factors with the strongest interaction in 2000, 2010, and 2020 were accumulated temperature \cap sunshine, accumulated temperature \cap sunshine, and GDP \cap land use, respectively, with q-values of 0.870, 0.876, and 0.428, respectively. The change in dominant factors indicates that the influence of human activities on vegetation growth in central and southern China is gradually increasing.



Figure 13. Cont.



Figure 13. Interaction factors: (a1) Northeast China (2000); (a2) Northeast China (2010); (a3) Northeast China (2020); (b1) North China (2000); (b2) North China (2010); (b3) North China (2020); (c1) East China

(2000); (c2) East China (2010); (c3) East China (2020); (d1) Northwest China (2000); (d2) Northwest China (2010); (d3) Northwest China (2020); (e1) Southwest China (2000); (e2) Southwest China (2010); (e3) Southwest China (2020); (f1) Central China (2000); (f2) Central China (2010); (f3) Central–South China (2020).

4. Discussion

4.1. Causes of Spatial and Temporal Changes of Terrestrial Vegetation in China over the Past 20 Years

This study employs linear regression for trend analysis, which offers the advantages of producing more intuitive and clear analysis results and being computationally efficient, especially for large-scale datasets. It can also be used for feature selection. However, linear regression is not suitable for analyzing nonlinear trends and is sensitive to outliers. In contrast, the Mann–Kendall test is a non-parametric method that does not require samples to adhere to specific distributional assumptions and is robust against outliers. It is applicable to categorical and ordinal variables, demonstrating strong versatility and computational simplicity. It is particularly useful for detecting nonlinear trends in vegetation cover. Therefore, this method can be effectively applied in future research endeavors.

In the regions of China, the NDVI generally exhibits higher values in the southeast and northeast and lower values in the northwest. This pattern may be related to the characteristics of crops grown in different regions; for instance, spring wheat is cultivated in the northeast, while winter wheat is grown in Qinghai. Additionally, studies show that the average NDVI varies with changes in altitude. Changes in the vegetation NDVI can explain the cyclical patterns of vegetation growth. Research indicates that August is the period when vegetation growth is most vigorous throughout the year. In spring, as temperatures warm and sunlight intensifies, vegetation vigor is restored in most parts of the country, leading to a significant increase in the NDVI. During summer, favorable climatic conditions lead to peak vegetation growth. However, in regions like southern Xinjiang and western Inner Mongolia, there is a decrease in NDVI values. This is because vegetation in these areas shows a significant correlation between the NDVI and temperature in spring and autumn, while the correlation between the NDVI and temperature in summer is not significant [14].

In our study, China's vegetation coverage gradually decreased [15]. In southern China, the climate was dominated by a monsoon climate. In summer, it was characterized by high temperature, rain, and humidity. The warm and humid air flowing from the Pacific Ocean penetrated into southern China, which was conducive for plant growth and promoted higher vegetation coverage [16]. In Northeast China, high vegetation coverage areas were mainly located in the Northeast Plain and other regions. The climate was cold and humid in winter, which was conducive to the accumulation of organic matter. In addition, it was warm and rainy in summer, which was helpful for the decomposition of organic matter and was suitable for the formation of fertile black soil. The fertile black soil provided sufficient nutrient conditions for vegetation growth [17]. In addition, the northeastern region is surrounded by mountains on three sides and opens to the south, which is conducive to the entry of marine water vapor and more precipitation. At the same time, the latitude of the region is high, evaporation is low, a permafrost layer exists, surface water is abundant, the climate is relatively humid, and a cold and humid environment is formed, which makes it easy to form a large number of forests [18]. Low vegetation coverage is mainly distributed in the first step of China. There is a vast Taklimakan Desert in this area. The Qinghai–Tibet Plateau has a high terrain. The temperature difference between day and night in the desert area is large, precipitation is scarce, sandy soil has difficulty fixing to the roots of ordinary crops, the altitude of the Qinghai–Tibet Plateau is high, the temperature is low, and the water vapor from the Pacific Ocean and the Indian Ocean is difficult to reach. It is not suitable for vegetation growth [19].

From 2000 to 2020, the vegetation coverage in different regions of China showed different degrees of increase, which may be related to the national macro-control. As early

as 2010, the state issued a reply on the outline of the national forest land protection and utilization plan, requiring good forest land protection [20]. Among them, the vegetation NDVI of central and southern regions had the highest increase of 0.0039, which might be related to the local positive response to the national policy of returning farmland to forest and grassland [21].

4.2. The Dominant Influencing Factors of Vegetation Change in China and Its Reasons for Change

In 2000, the dominant factor affecting vegetation change in Northeast China was precipitation. The southeast of Northeast China was dominated by mountains, with high terrain and low temperatures. Precipitation was mainly in the form of snow, which was not conducive to vegetation growth [22]. The dominant influencing factor of the NDVI in 2010 and 2020 was land use change due to the continuous improvement of the urbanization level. There is a dual relationship between urbanization and vegetation growth. Reasonable urbanization could enhance vegetation coverage, such as the implementation of reasonable protection of forest land and other policies in the city [23]. Unreasonable urbanization, such as the reclamation of wasteland, could enhance the level of urbanization and might cause a certain degree of damage to the original forest land and reduce vegetation coverage [24]. In North China, the dominant factor affecting vegetation change was precipitation. The region is located in a semi-humid and semi-arid area. Because vegetation growth is extremely sensitive to climate change, vegetation changes greatly with precipitation. Moisture is very important to the growth of vegetation in this area. Precipitation is relatively scarce in the growing season, which makes precipitation play a leading role in the growth of vegetation in this area [25]. In 2000, 2010, and 2020, the dominant factors affecting vegetation change in East China were land use, GDP, and land use, which were all related to human activities. As one of the most economically developed areas in China, human activities had an important impact on vegetation change in East China. The impacts of human activities on vegetation change were double-edged. Reasonable conversion of farmland to forest was conducive to vegetation restoration, while human deforestation, unreasonable reclamation of wasteland, and the improvement of the urbanization level reduced vegetation coverage [26]. The dominant factor of vegetation change in Northwest and Southwest China was precipitation. Northwest China was facing serious environmental problems, such as a shortage of water resources and a fragile ecological environment. Drought and water shortage were among the important problems restricting the economic and social development of the region. Water resources were one of the important conditions for vegetation growth. A lack of water resources greatly limits the growth of vegetation [27]. In the Qinghai–Tibet Plateau, the terrain was high and precipitation was scarce. The increase in precipitation promoted the growth of vegetation. In Yunnan, precipitation was abundant, and excessive precipitation led to severe soil erosion, which finally inhibited the growth of vegetation [28]. In 2000, 2010, and 2020, the dominant factors affecting vegetation change in the central and southern regions were precipitation and land use, which gradually shifted from climatic factors to human activity factors. With the continuous improvement of human living standards and urbanization levels, the influence of human activities on vegetation growth and change has gradually become stronger.

5. Conclusions

Based on the MODIS NDVI time series data set, this study used a barycenter model, time lag effect analysis method, partial correlation analysis, and geographical detector to explore the spatial and temporal evolution pattern of the vegetation NDVI in different ecological sub-regions of China and analyzed the time lag and dominant driving factors affecting the vegetation NDVI change. The main conclusions are as follows:

- (1) The vegetation coverage in mainland China showed a decreasing trend from east to west.

- (2) The vegetation coverage of the six sub-regions showed an increasing trend over the past 20 years, with the highest increase in Central–South China, which was 0.0039, and the lowest increase in East China, which was 0.002.
- (3) The gravity center in Northeast China showed a trend of migration to the northwest. The gravity center in North China, East China, and Central–South China showed a trend of migration to the southwest. The gravity center in Northwest China showed a trend of migration to the southeast. The gravity center in Southwest China showed a trend of migration to the southeast.
- (4) During the period from 2000 to 2020, vegetation cover levels showed an upward trend.
- (5) The lag times of different vegetation types varied across different regions.
- (6) Precipitation was the dominant factor that had the strongest influence on vegetation cover in Northeast China, North China, Northwest China, and Southwest China. Land use and GDP had the strongest influences on vegetation cover in East China. Precipitation and land use had the strongest influences on vegetation cover in Central–South China.

Author Contributions: Conceptualization, methodology, and writing—original draft preparation, B.G. and M.X.; investigation, supervision, project administration, and funding acquisition, R.Z., W.L. and J.Y. All authors have read and agreed to the published version of the manuscript.

Funding: This research was funded by the National Natural Science Foundation of China (grant numbers: 42101306, 42301102, 42071419), the Scientific Innovation Project for Young Scientists in Shandong Provincial Universities (grant number: 2022KJ224), the Natural Science Foundation of Shandong Province (grant number: ZR2021MD047), and the Agricultural Science and Technology Innovation Program (grant number CAAS-ZDRW202201).

Data Availability Statement: The data that support the findings of this study are available from Bing Guo upon reasonable request.

Conflicts of Interest: The authors declare no conflicts of interest.

References

1. Yan, M.; He, L.; Wang, S.J.; Zheng, M.G.; Sun, L.Y.; Xu, J.X. NDVI-based multi-time scale vegetation cover change in the Yellow River Basin from 1982 to 2012. *Sci. Soil Water Conserv. China* **2018**, *16*, 86–94.
2. Wang, W.; Alim, S.; Gilili, A. The spatio-temporal variation characteristics of NDVI and its driving factors in Central Asia based on the geo-detector model. *Remote Sens. Land. Resour.* **2019**, *31*, 32–40.
3. Xia, Z.H. Research on Vegetation Dynamic Change Based on NDVI Time Series. Master’s Thesis, Beijing Forestry University, Beijing, China, 2007.
4. Lu, J.Q.; Meng, F.H.; Luo, M.; Chen, H.G. The effects of meteorological drought and hydrological drought changes on vegetation NDVI in the Inner Mongolia section of the Yellow River Basin. *People’s Pearl River* **2024**, *45*, 1–19.
5. Wang, Y.K.; Liu, P.D.; Liu, J.T.; Zhang, D.; Wang, L.X.; Huang, L. Analysis of Spatiotemporal Changes in Ecological Environment Quality of the Yellow River Delta Based on Modified Remote Sensing Ecological Index. *J. Ecol. Rural. Environ.* **2024**, *6*, 1–17.
6. Shen, Z.A.; Wu, J.; Li, C.B. Spatial-temporal variation characteristics and driving forces of vegetation coverage in Hexi inland river basin from 2000 to 2020. *Chin. Desert.* **2024**, *44*, 119–127.
7. Mason, T.J.; Honeysett, J.; Thomas, R.F. Monitoring vital signs: Wetland vegetation responses to hydrological resources in the Macquarie Marshes NSW, Australia. *Austral. Ecol.* **2022**, *47*, 167–178. [[CrossRef](#)]
8. Vahagn, M.; Garegin, T.; Shushanik, A.; Fabio, D.A. Relationships between NDVI and climatic factors in mountain ecosystems: A case study of Armenia. *Remote. Sens. Appl.* **2019**, *14*, 90–114.
9. Lv, X.; Wang, J.L.; Kang, H.L.; Zhao, Q.; Han, X.H.; Wang, Y.J. Study on the spatio-temporal variation of grass yield in Sanjiangyuan region from 2006 to 2015 based on MODIS NPP. *J. Nat. Resour.* **2017**, *32*, 1857–1868.
10. He, K.D.; Sun, J.; Chen, Q.J. Effects of climatic factors and soil texture on grassland net primary productivity and precipitation use efficiency on the Qinghai-Tibet Plateau. *Lawn. Sci.* **2019**, *36*, 1053–1065.
11. Li, M.L.; Yin, L.C.; Zhang, Y.; Su, X.K.; Liu, G.H.; Wang, X.F.; Ao, Y.; Wu, X. Study on the temporal and spatial changes and driving factors of vegetation cover in Southwest China based on MODIS-EVI. *Acta Ecol. Sin.* **2021**, *41*, 1138–1147. [[CrossRef](#)]
12. Zhu, J.Y. Spatiotemporal Variation and Driving Factors of NDVI in Raohe River Basin from 2000 to 2020. Master’s Thesis, Jiangxi Agricultural University, Nanchang, China, 2023.
13. Wang, J.F.; Xu, C.D. Geographical detector: Principle and prospect. *Acta. Geogr. Sin.* **2017**, *72*, 116–134.
14. Du, J.Q.; Gao, Y.; Jiaerheng, A.H.T.; Zhao, C.X.; Fang, G.L.; Yuan, X.J.; Yin, J.Q.; Shu, J.M. Spatio-temporal patterns and driving factors of vegetation growth anomalies in Xinjiang over the last three decades. *Acta Ecol. Sin.* **2016**, *36*, 1915–1927.

15. Jin, K. Spatial and Temporal Changes of Vegetation Coverage in China and Its Relationship with Climate and Human Activities. Doctoral dissertation, Northwest A&F University, Yangling, China, 2019.
16. Jiang, P. Analysis of Vegetation Cover Change and Its Sensitivity to Climate Change in China from 1982 to 2015. Ph.D. Thesis, Lanzhou university, Lanzhou, China, 2023.
17. Zhu, Y.X. The value of black land. *Environ. Econ.* **2020**, *17*, 72.
18. Gao, J.W.; Liu, J.Y.; Zhang, Q.J.; Zhao, F.S.; Cui, X.X.; Wang, Q. The impact of forest ecological formation in Daxing'anling on China's ecological environment and protection countermeasures. *IM. Sci. Tech. Econ.* **2003**, *22*, 24–25.
19. Du, Y.Z.; Cui, Y.; Ni, J. Spatio-temporal variation analysis of vegetation NDVI in growing season of Tibetan Plateau based on MODIS data. *J.UZZ.* **2024**, *41*, 49–55.
20. Qian, S.; Cui, X.J.; Jiang, Y.Q. Interpretation of QX/T 494-2019. Land Vegetation Meteorological and Ecological Quality Inspection and Evaluation Grade. *Stand. Sci.* **2022**, *7*, 125–134.
21. Liu, Y.B.; Liu, B.Y.; Cheng, C.; Zhang, J.Q.; Lu, S.J. Analysis of spatial and temporal changes and influencing factors of vegetation coverage in Yulin City in the past 20 years. *J. Soil. Water. Conserv.* **2022**, *36*, 197–208+218.
22. Xie, Y.; Wang, S.; Wang, H.Y.; Yang, X.; Zhang, F.L.; Wang, N.; Tao, F. The temporal and spatial variation characteristics of NDVI and its response to climate factors in the three northeastern provinces. *J. Meteorol. Environ.* **2024**, *40*, 71–78.
23. Ma, L. Research on ecological management path in soil and water conservation and desertification control. *Marit. Safety* **2023**, *43*, 66–68.
24. Wang, H. Oasis urbanization and water and soil resources utilization benefit coordination degree analysis. NWNNU. 2014.
25. Jiang, H.X.; Dong, W.J. Effects of climate change and human activities on vegetation NDVI in North China. *Plateau. Meteorol.* **2024**, *43*, 1–17.
26. Pei, Z.L.; Cao, X.J.; Wang, D.; Li, D.; Wang, X.; Bai, A.Y. Spatio-temporal variation characteristics of vegetation coverage in Inner Mongolia and its response to human activities. *Arid. Zone. Res.* **2024**, *41*, 629–638.
27. Tian, J.X. Research on the Evolution Trend of Warm and Humid Climate in Northwest China and Its Impact on Vegetation Restoration. Ph.D. Thesis, Nanjing Forestry University, Nanjing, China, 2024.
28. Liu, Y.T.; Wang, L.; Li, X.H.; Guo, L. Analysis of spatial and temporal changes and influencing factors of vegetation coverage in Southwest China from 2000 to 2020. *Plateau. Meteorol.* **2024**, *43*, 264–276.

Disclaimer/Publisher's Note: The statements, opinions and data contained in all publications are solely those of the individual author(s) and contributor(s) and not of MDPI and/or the editor(s). MDPI and/or the editor(s) disclaim responsibility for any injury to people or property resulting from any ideas, methods, instructions or products referred to in the content.